初代星起源コンパクト連星からの重力波

衣川　智弥

東大宇宙線研究所

The beginning of Gravitational wave astronomy

- Gravitational wave detectors

KAGRA

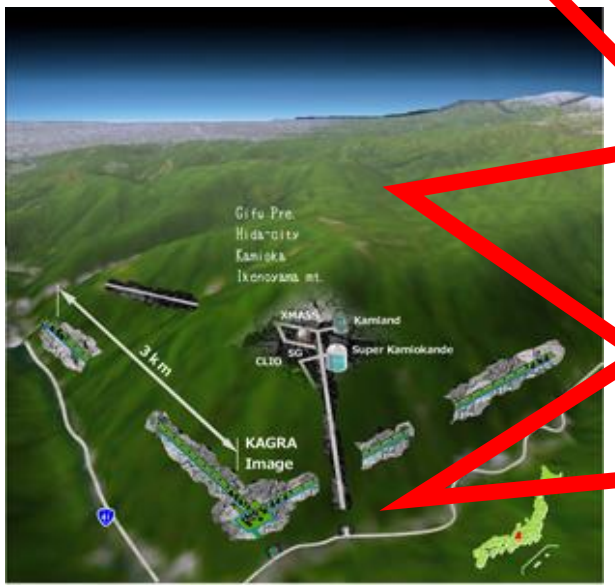

©KAGRA

Advanced LIGO

©LIGO

Advanced VIRGO

©VIRGO

GW150914

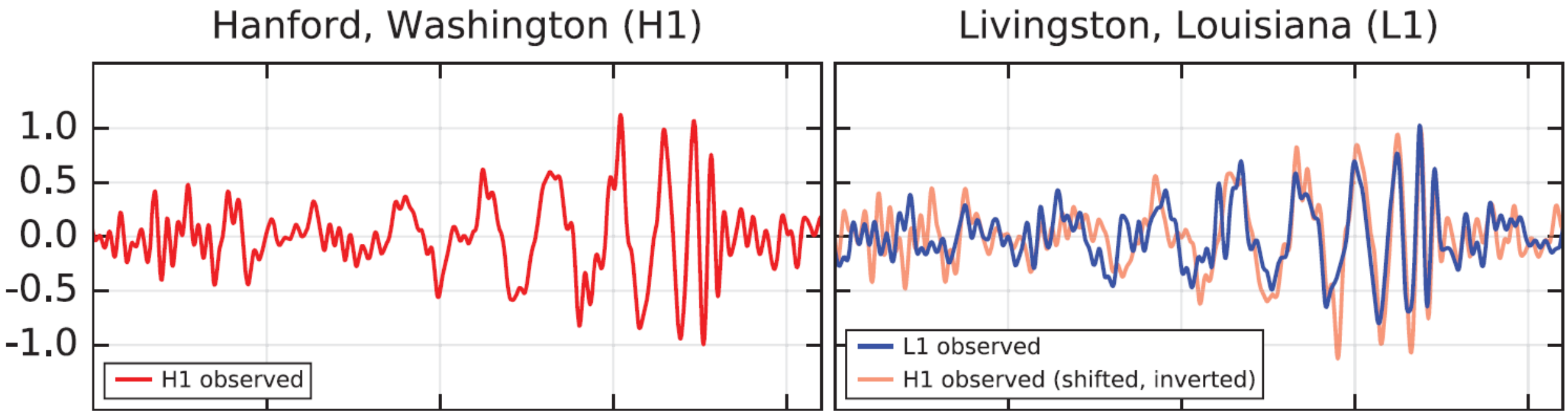
Hanford, Washington (H1)
Livingston, Louisiana (L1)
1.0
0.5
0.0
-0.5
-1.0
H1 observed
L1 observed
H1 observed (shifted, inverted)

GW150914

PRL 116, 061102 (2016) Selected for a Viewpoint in *Physics* PHYSICAL REVIEW LETTERS week ending 12 FEBRUARY 2016

Observation of Gravitational Waves from a Binary Black Hole Merger

B. P. Abbott *et al.*[*]
(LIGO Scientific Collaboration and Virgo Collaboration)
(Received 21 January 2016; published 11 February 2016)

On September 14, 2015 at 09:50:45 UTC the two detectors of the Laser Interferometer Gravitational-Wave Observatory simultaneously observed a transient gravitational-wave signal. The signal sweeps upwards in frequency from 35 to 250 Hz with a peak gravitational-wave strain of 1.0×10^{-21}. It matches the waveform predicted by general relativity for the inspiral and merger of a pair of black holes and the ringdown of the resulting single black hole. The signal was observed with a matched-filter signal-to-noise ratio of 24 and a false alarm rate estimated to be less than 1 event per 203 000 years, equivalent to a significance greater than 5.1σ. The source lies at a luminosity distance of 410^{+160}_{-180} Mpc corresponding to a redshift $z = 0.09^{+0.03}_{-0.04}$. In the source frame, the initial black hole masses are $36^{+5}_{-4} M_\odot$ and $29^{+4}_{-4} M_\odot$, and the final black hole mass is $62^{+4}_{-4} M_\odot$, with $3.0^{+0.5}_{-0.5} M_\odot c^2$ radiated in gravitational waves. All uncertainties define 90% credible intervals. These observations demonstrate the existence of binary stellar-mass black hole systems. This is the first direct detection of gravitational waves and the first observation of a binary black hole merger.

GW150914

- 36太陽質量+29太陽質量の連星ブラックホール（BBH)
- 一方、従来X線連星で観測されてきたBH候補天体は～10太陽質量
  →今まで観測されたBHより2-3倍重い

このBBHの起源を説明するために様々な説が提唱されている

- 低金属量星(種族Ⅱ星)起源
- 初代星（種族Ⅲ星）起源
- 星団起源
- 原始BH起源
- ・・・・・・

連星として生まれてきた
低金属な星起源

連星として生まれる星

- 恒星のうち連星である者の割合は多い

Example

Milky way young open clusters

71 O stars　fbinary=69+/-9% (P<3200days) Sana et al. 2012

30 Doradus (Tarantula Nebula)

362 O stars fbinary=51+/-4%(P<3200days) Sana et al. 2013

©star wars

なぜ低金属量星を考えるのか?

- もし、BHが種族I (=Solar metal stars)だったら？
  →重くても恒星風で質量を失いすぎる
  そもそも質量分布が$M^{-2.35}$なうえ、軽い星（～太陽質量）が多い

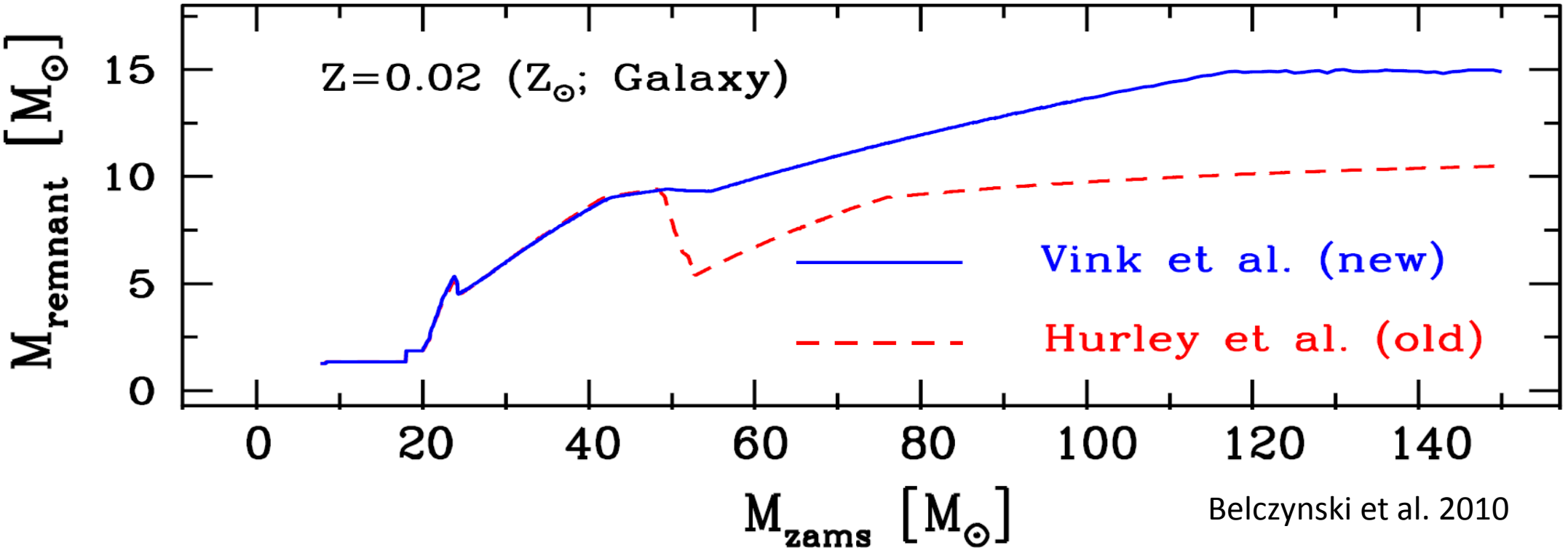

Belczynski et al. 2010

低金属量星の場合

- 種族Ⅱ (Z<0.1Zsun)
  典型的な質量は種族Iと同等
  しかし、低金属な分、恒星風が弱い
  →質量失いにくい
- 初代星 (No metal)
  典型的な質量が種族I,IIに比べ重い
  MpopIII~10-100Msun
  恒星風が効かない

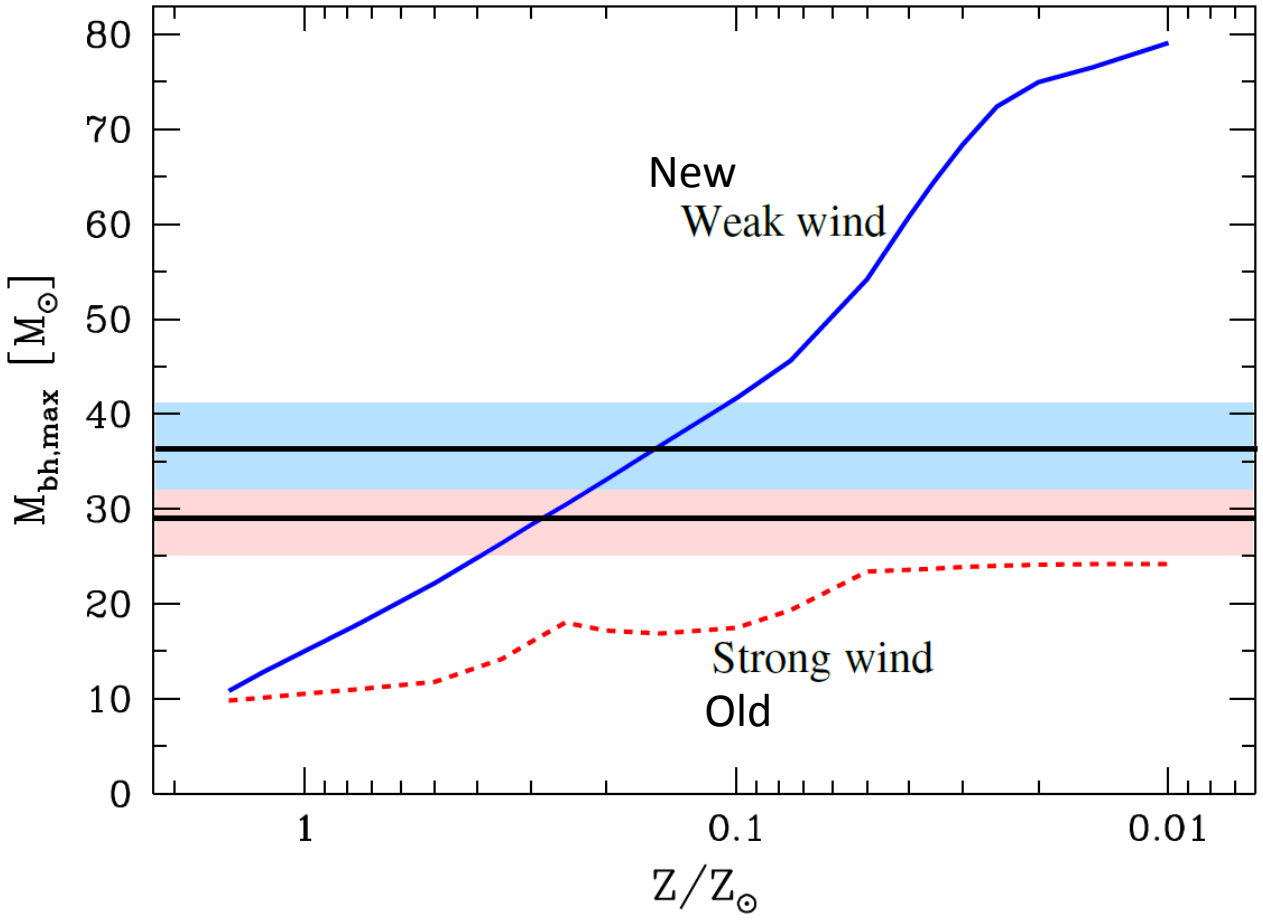

Minitial: 8Msun<M<150Msun
Single stellar evolution
with 2 stellar wind models.
(Belczynski et al.2010,Abbot et al.2016)

金属量による（単独）星の違い

	種族I	種族II （低金属量星）	種族III （初代星）
金属量	太陽と同等	太陽の10%以下	0
質量	～1太陽質量	～1太陽質量	~10-100太陽質量
恒星風による質量損失	効く	効きづらい	全く効かない

Total mass distribution of BBH which merge within the Hubble time

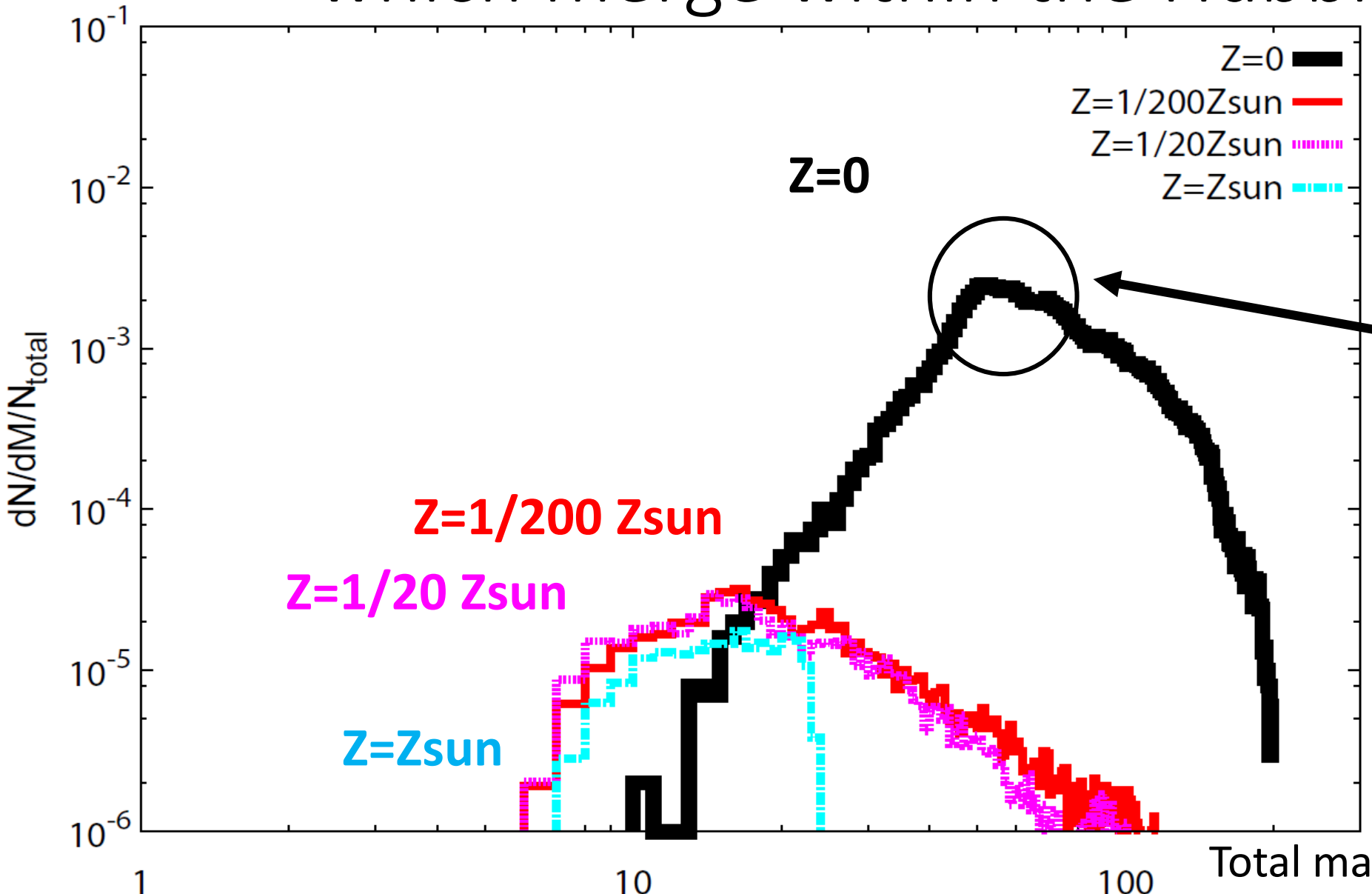

Typical total mass

M～60 $M_\odot$

(30 $M_\odot$ +30 $M_\odot$)

Kinugawa et al. 2014, 2016

e.g. Pop I, Pop II (Z=0.02,0.001,0.0001)
IMF:Salpeter (1Msun<M<140Msun)
Typical mass ～10 $M_\odot$

なにがBBHの質量分布を決めるのか?

- 単独星の進化（生まれたときの質量、恒星風による質量損失）
- 連星相互作用

(Mass transfer, Common envelope)

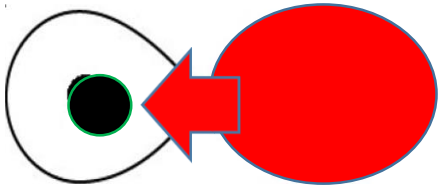

Mass transfer

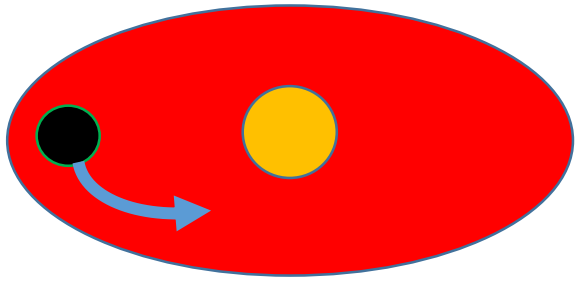

Common envelope

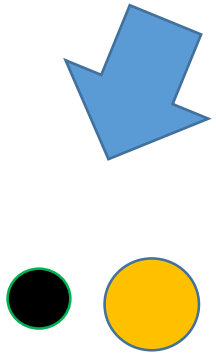

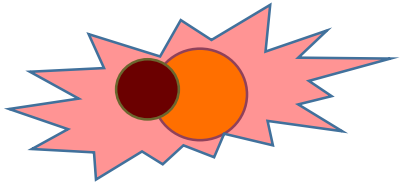

Close binary or merge

星の進化（HR図）

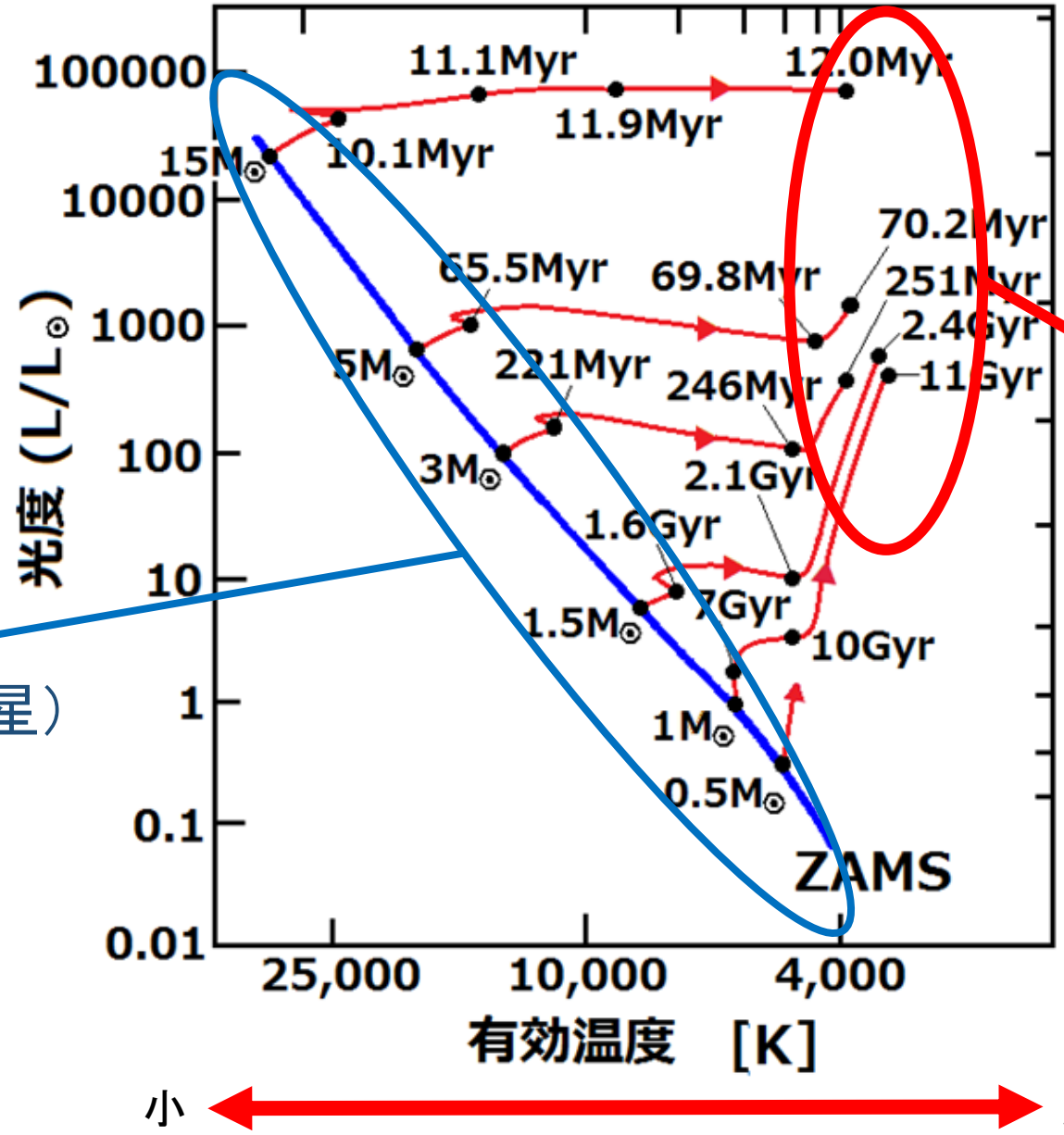

主系列星
（水素燃焼の星）

赤色巨星
Common envelope
になりやすい

小 ⟷ 大
半径

©http://astroexercise.wiki.fc2.com/wiki/

なぜ初代星が 30MsunのBBHになるのか？

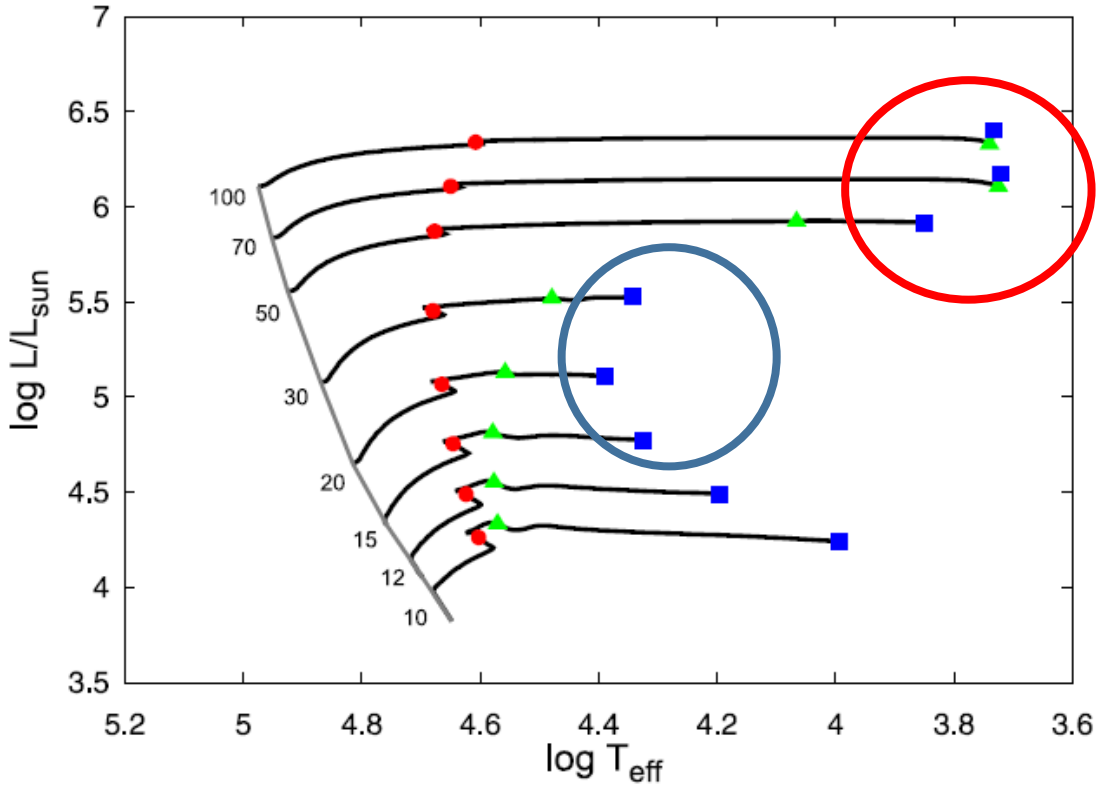

Figure 1. The Hertzsprung-Russell (HR) diagram for the Pop III stars of mass 10 $M_\odot \leqslant M \leqslant 100\ M_\odot$ using the data taken from Marigo et al. (2001). The number attached to each solid curve is the mass of each star in unit of $M_\odot$. The dashed line shows the ZAMS (Zero Age Main Sequence) stars. Red circles, green triangles and blue squares correspond to the beginning of He-burning, the end of the He-burning and the beginning of the C-burning, respectively.

- M>50Msun　赤色巨星
  →Mass transfer 不安定
  →common envelope
  →1/3~1/2 of initial mass (~25-30Msun)

- M<50Msun　青色巨星
  →Mass transfer 安定
  →mass loss が効きづらい
  →2/3~1 of initial mass (25-30Msun)

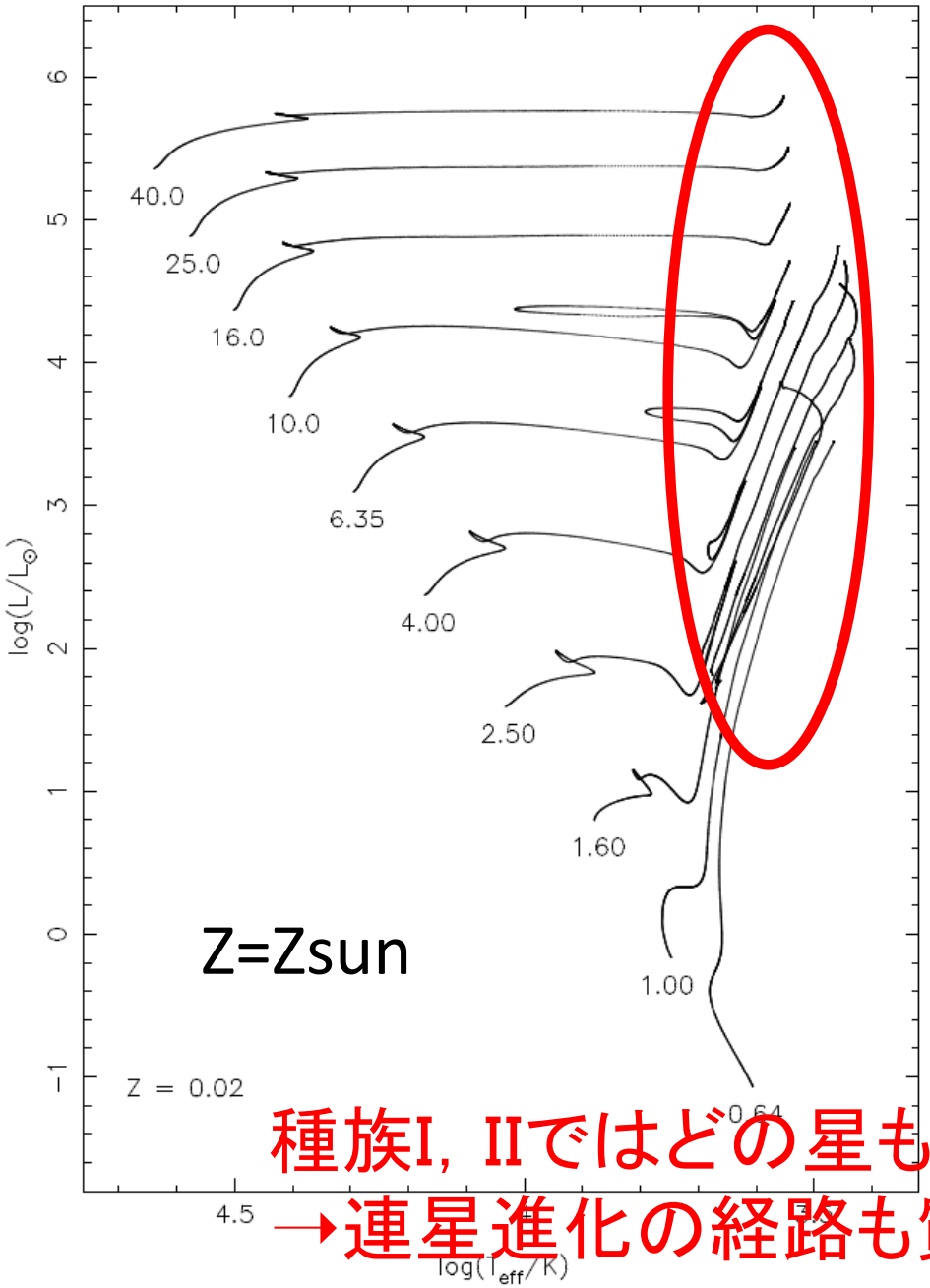

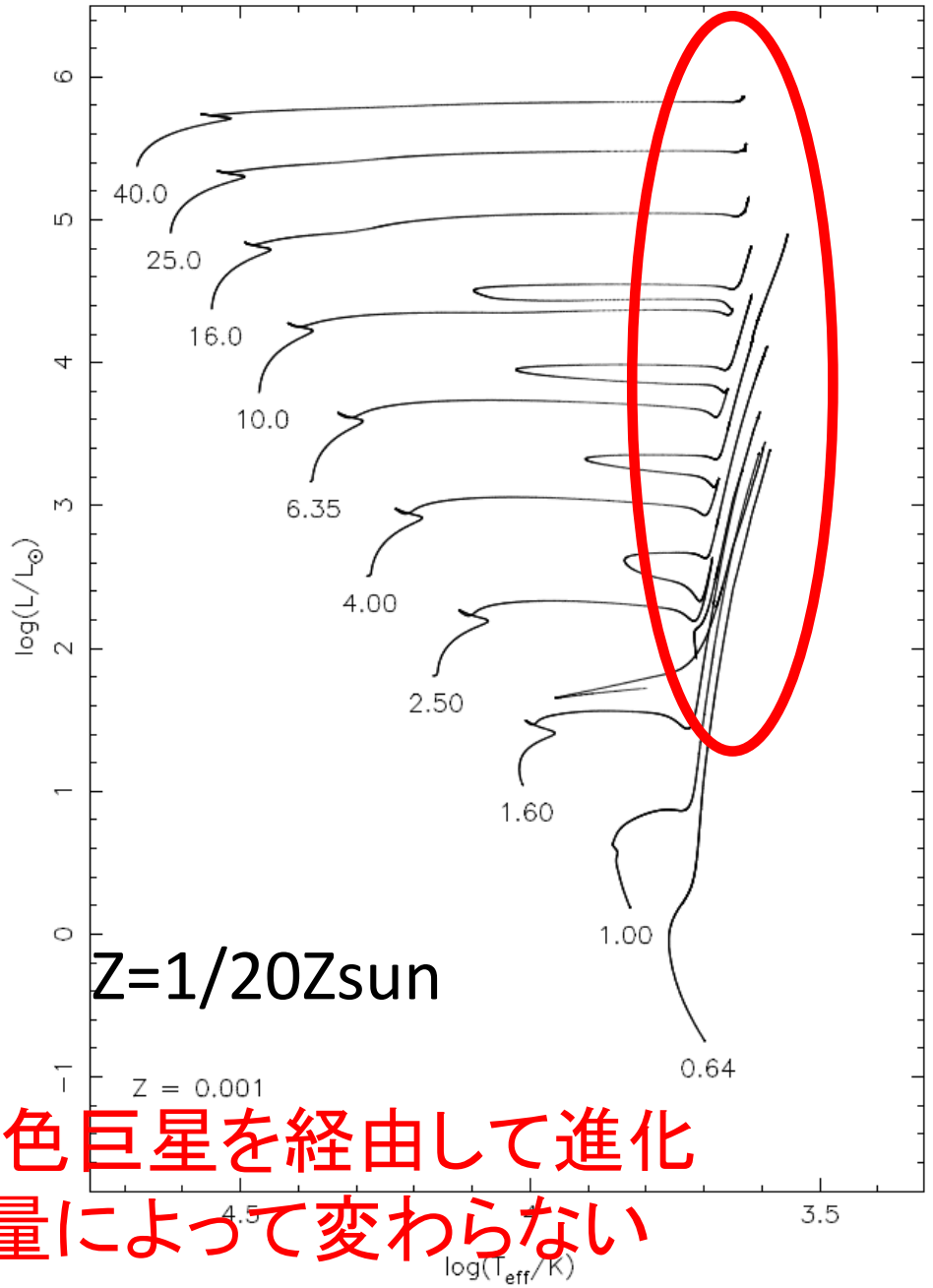

種族I，IIではどの星も赤色巨星を経由して進化
→連星進化の経路も質量によって変わらない

Figure 1. Selected OVS evolution tracks for $Z = 0.02$, for masses 0.64, 1.0, 1.6, 2.5, 4.0, 6.35, 10, 16, 25 and 40 $M_{\odot}$.

Figure 2. Same as Fig. 1 for $Z = 0.001$. The 1.0 $M_{\odot}$ post He flash track has been omitted for clarity.

Total mass distribution of BH-BH which merge within the Hubble time

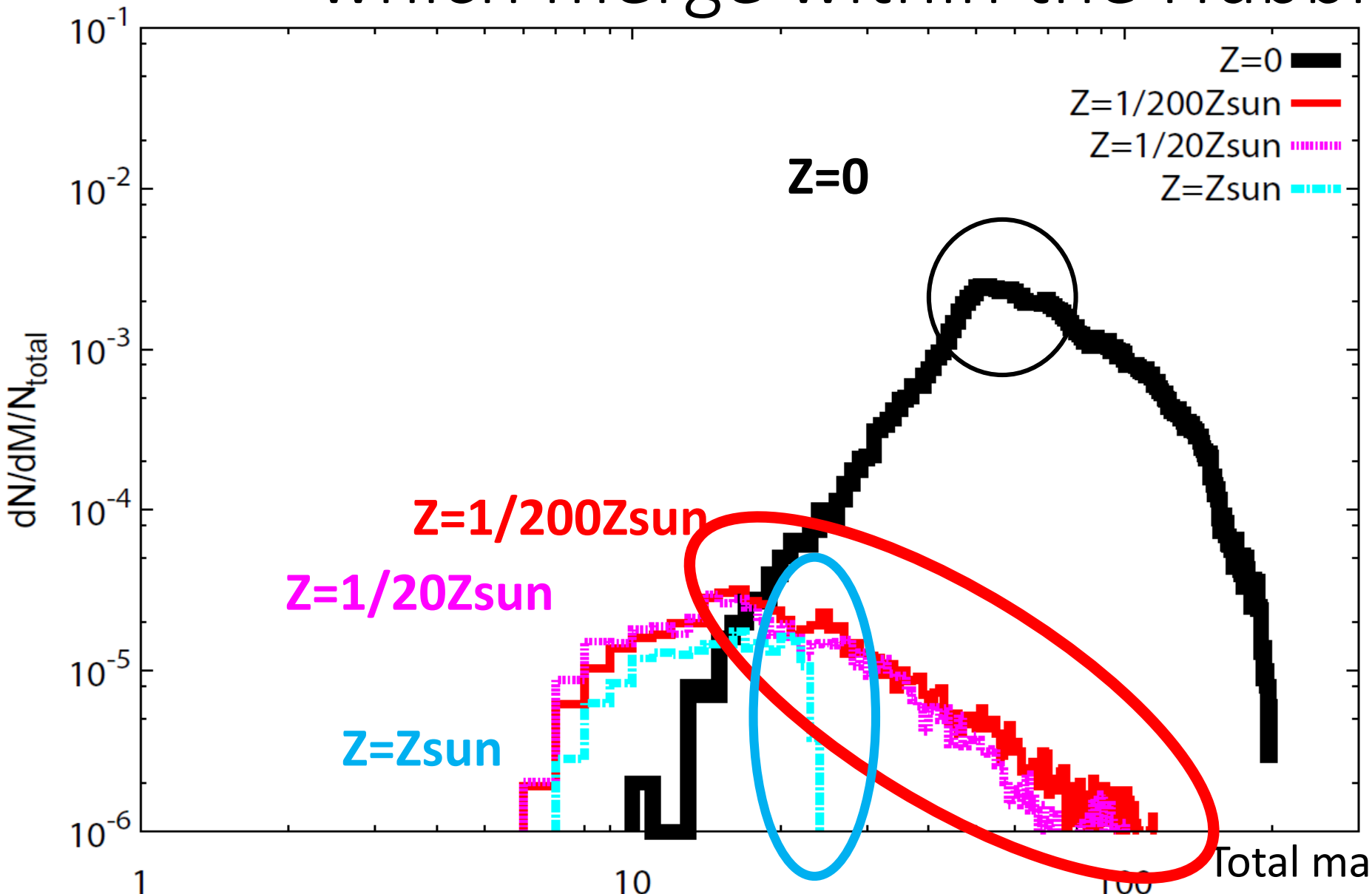

初代星起源BBHの質量分布は星の進化を反映

種族IIは初期質量分布を反映

種族Iは恒星風のせいで重いものができない

初代星起源のBBH

- 初代星が生まれる時期 z~10
- 重力波で合体するまでの時間~$10^{8\text{-}10}$yr
- <u>重力波源の累積を考慮する必要がある</u>
- 宇宙初期にできた星で現在合体するものが見られるかもしれない

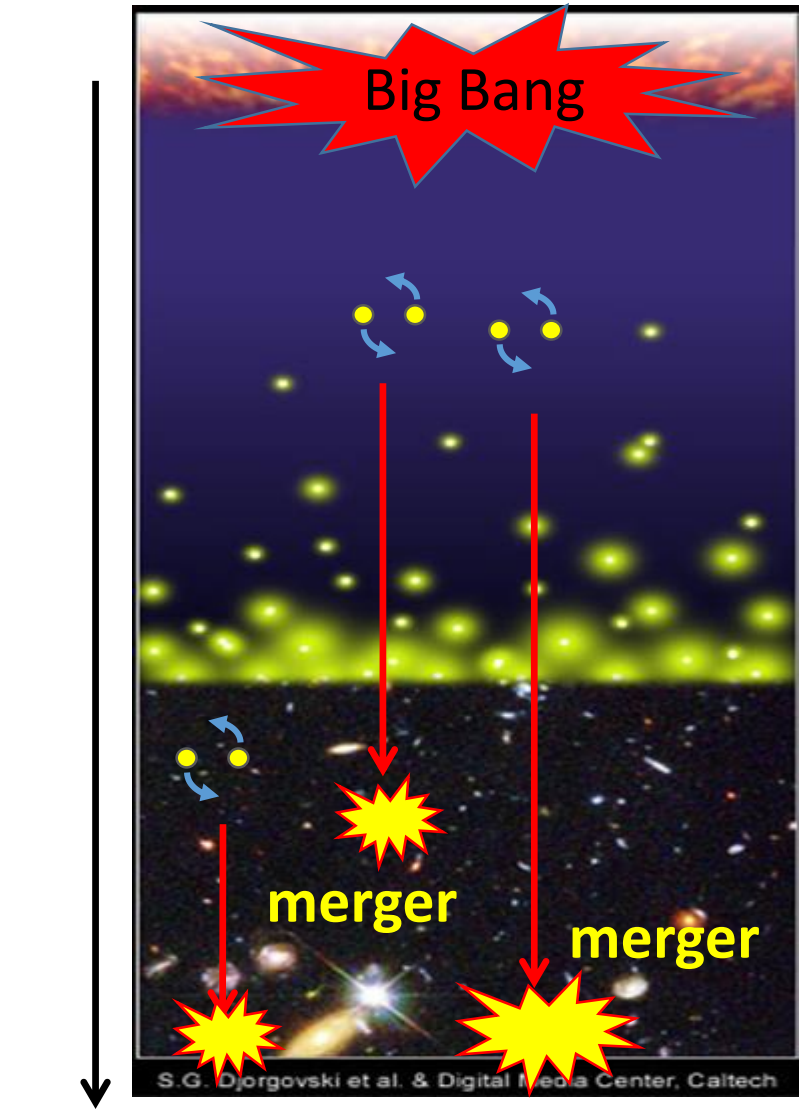

Djorgovski et al.&Degital Media Center

Pop III BBH?

ASTROPHYSICAL IMPLICATIONS OF THE BINARY BLACK-HOLE MERGER GW150914

ApJL Abbot. et al 2016

2014; Dominik et al. 2015).

On the extreme low-metallicity end, it has been proposed that BBH formation is also possible in the case of stellar binaries at zero metallicity (Population III [PopIII] stars; see Belczynski et al. 2004; Kinugawa et al. 2014). The predictions from these studies are even more uncertain, since we have no observational constraints on the properties of first-generation stellar binaries (e.g., mass function, mass ratios, orbital separations). However, if one assumes that the properties of PopIII massive binaries are not very different from binary populations in the local universe (admittedly a considerable extrapolation), then recently predicted BBH total masses agree astonishingly well with GW150914 and can have sufficiently long merger times to occur in the nearby universe (Kinugawa et al. 2014). This is in contrast to the predicted mass properties

連星進化の理論計算

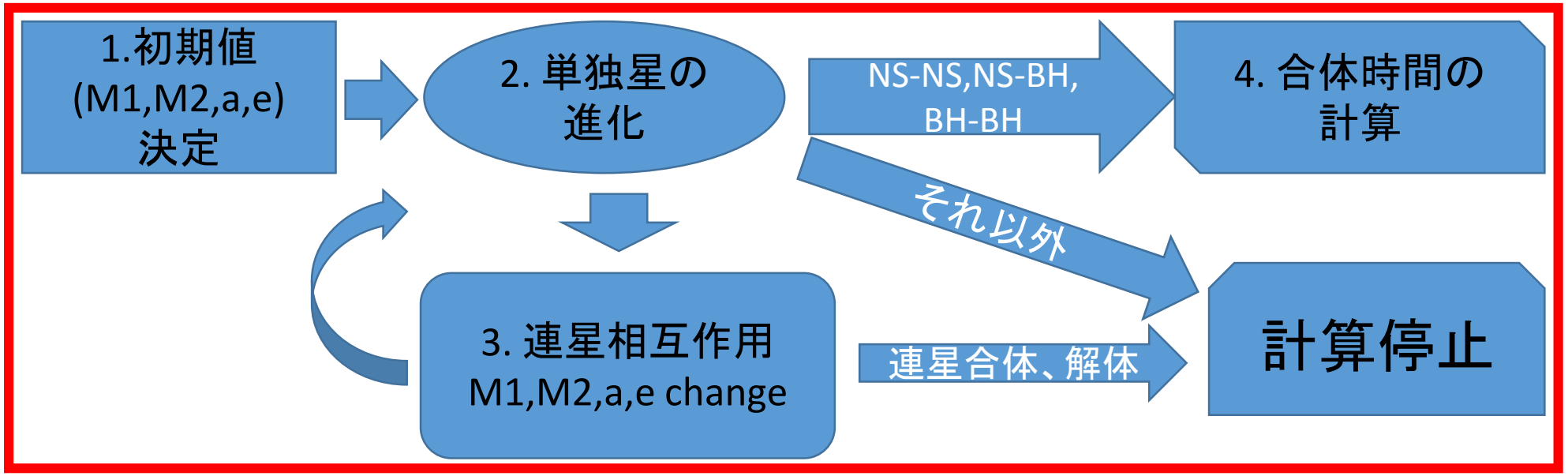

- 上記の連星計算をモンテカルロシミュレーションすることで連星の合体確率を計算する

連星相互作用

- Tidal friction
- Common envelope
- Mass transfer
- Supernova effect
- Gravitational radiation

Change
M1,M2,a, e

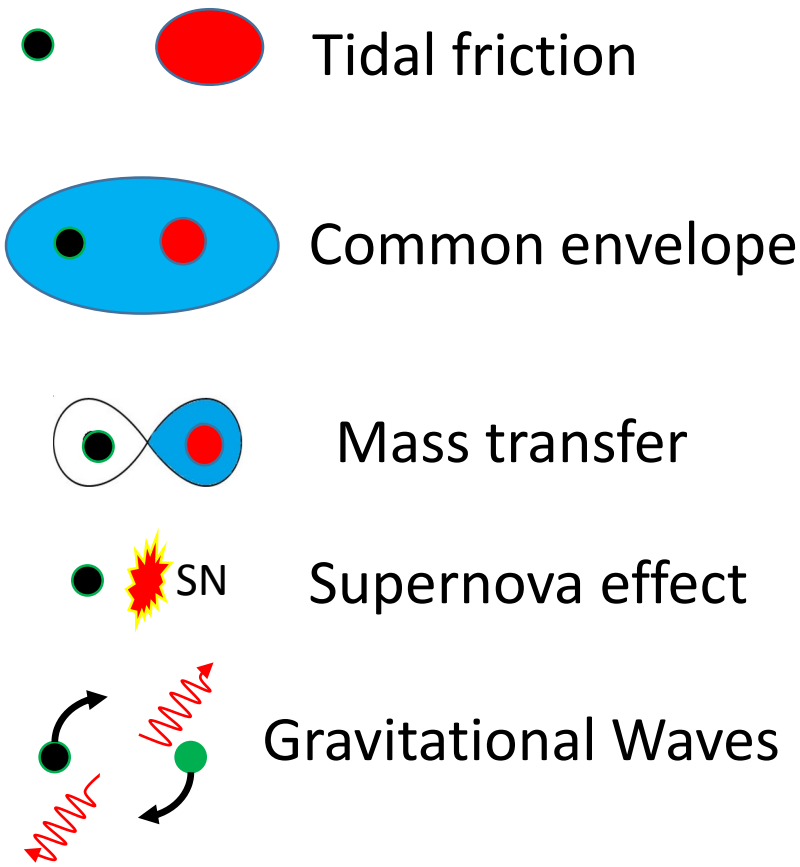

連星進化のパラメータは種族I連星と同様の値を仮定

初代星連星進化計算

10^6個の初代星連星について進化計算
初代星の進化はMarigo et al. (2001)を使用

- 初期分布関数(Standard model)

  M1 : P(M1)=const. (10 $M_\odot$<M<100 $M_\odot$)

  q=M2/M1 : P(q)=const. (10/M_1<q<1)

  a : P(a)∝1/a (a_{min}<a<$10^6 R_\odot$)

  e : P(e)∝e (0<e<1)

計算結果(Standard model)

10^6連星中のコンパクト連星数

	NSNS	NSBH	BHBH
形成数	0	185335	517067
合体数	0	50	115056

- 10^6個中一割が連星ブラックホールとして合体

Total mass distribution of BH-BH which merge within the Hubble time

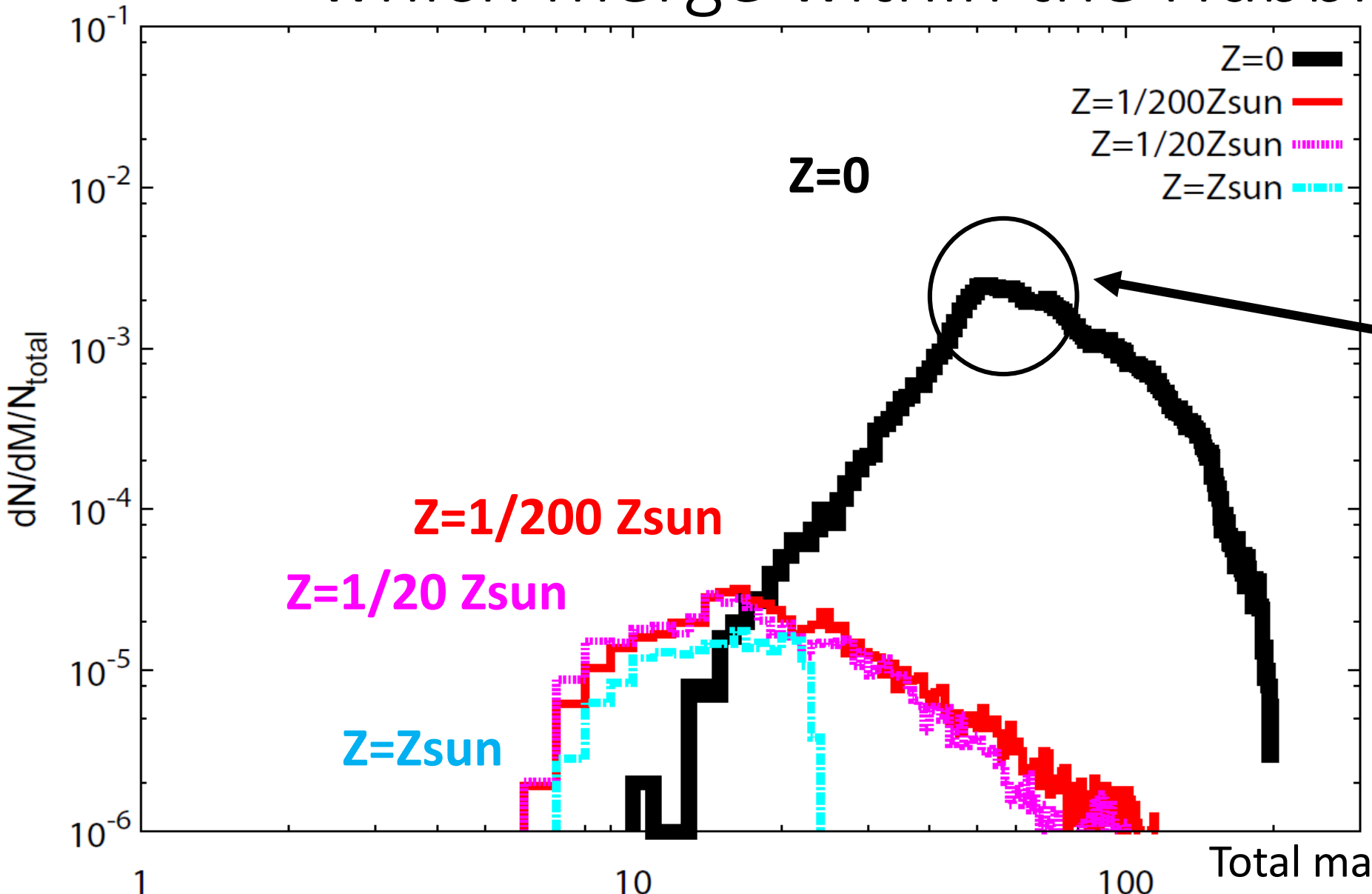

Typical total mass
M～60 $M_\odot$
(30 $M_\odot$ +30 $M_\odot$)
Kinugawa et al.
2014, 2016

e.g. Pop I, Pop II
(Z=0.02,0.001,0.0001)
IMF:Salpeter
(1Msun<M<140Msun)
Typical mass ～10 $M_\odot$

The star formation rate of Pop III

合体率を計算するために

- いつ初代星が生まれたのか?
- どのくらいの数が生まれたのか?

⇒初代星の星形成率が必要

初代星の星形成率として

右のものを使用

de Souza et al. 2011

$SFR_{peak} \sim 10^{-2.5}$ [$M_\odot$ yr^{-1} Mpc^{-3}]

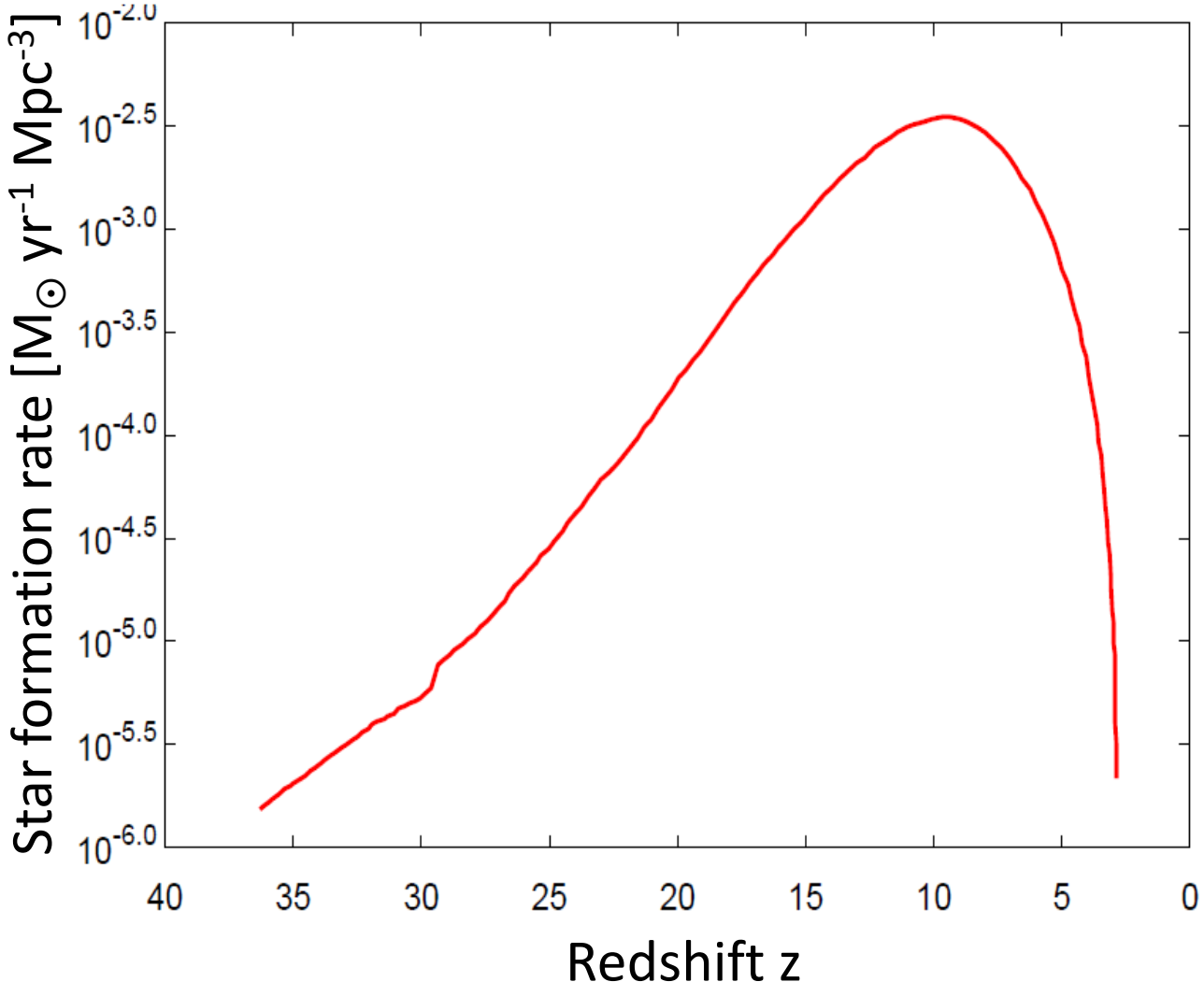

(de Souza et al. 2011)

初代星BBHの合体率

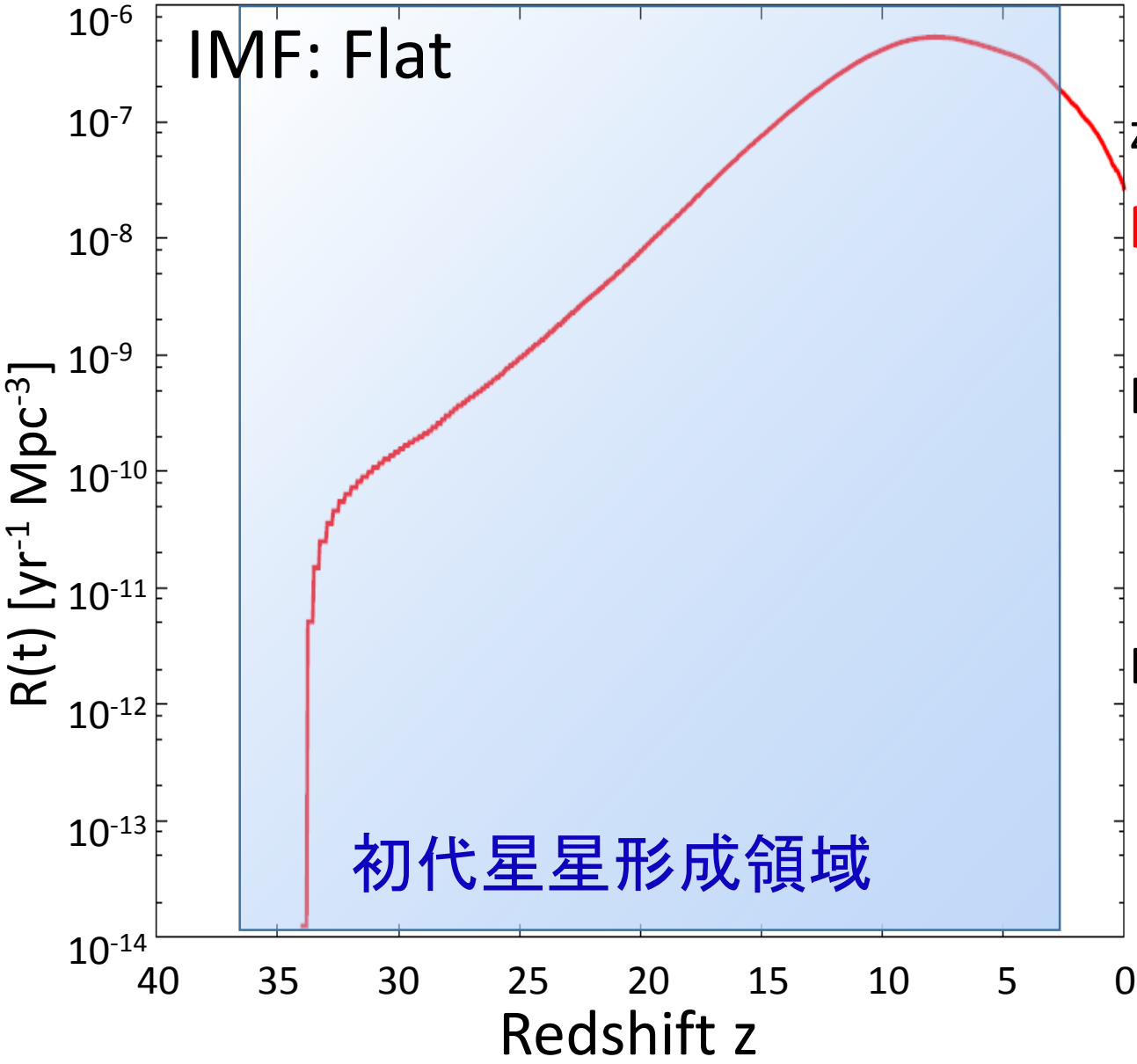

z=0での初代星BBH合体率

$$R \sim 2.5 \times 10^{-8} \left(\frac{SFR_{peak}}{10^{-2.5}}\right)\left(\frac{f_b/(1+f_b)}{0.33}\right) \underline{Err_{sys}}$$

$[yr^{-1}\ Mpc^{-3}]$

Err_{sys}: 以下の要因によるsystematic error

- binary evolution treatment
- initial distribution functions

$Err_{sys} = 1$はstandard modelの時に対応

Detection range of KAGRA and Adv. LIGO

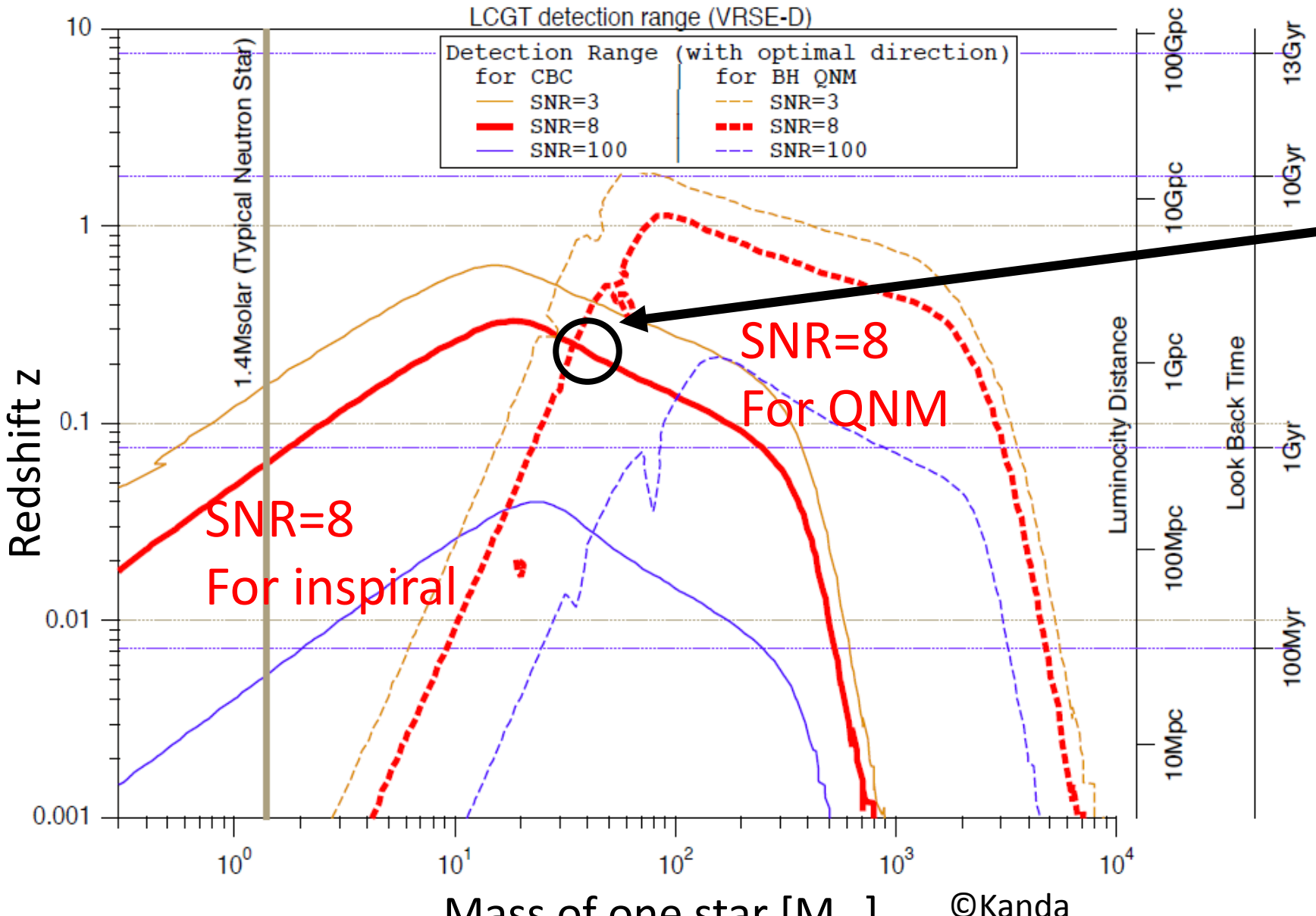

M_{BH}～30$M_\odot$
SNR=8

Luminocity distance
～1.5 Gpc

Redshift z～0.28

Inspiral and QNM

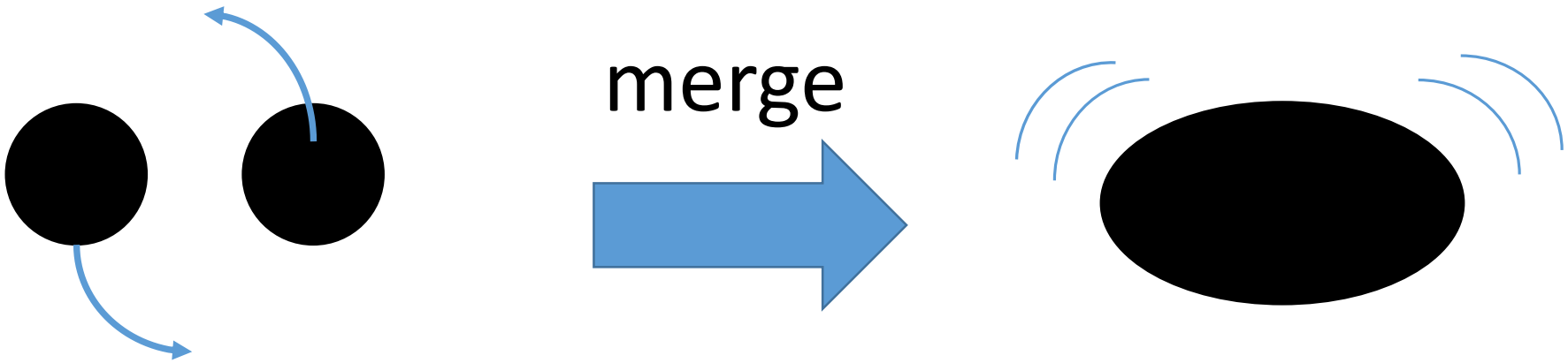

inspriral

QNM

Detection range of KAGRA and Adv. LIGO

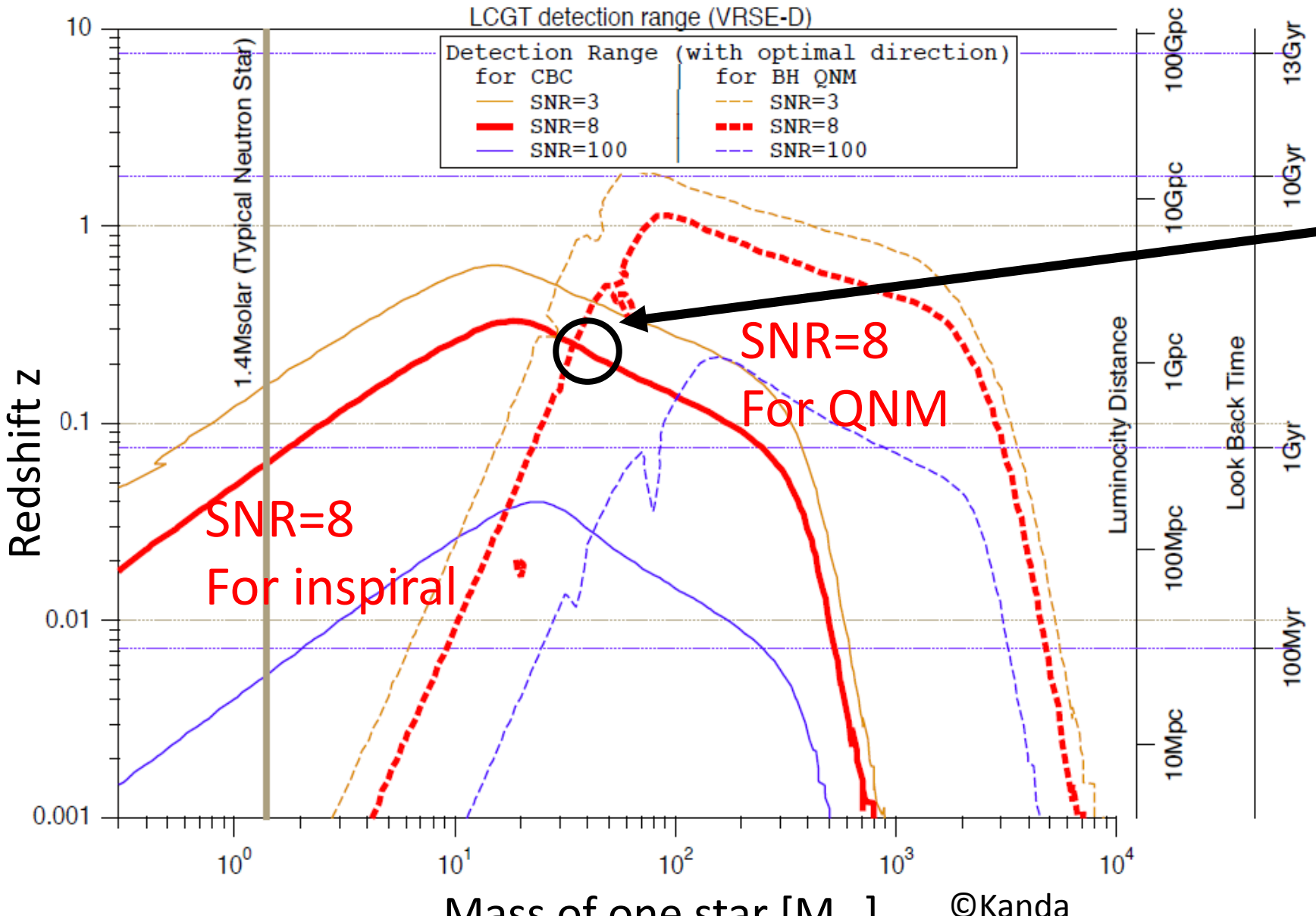

M_{BH}～30$M_\odot$
SNR=8

Luminocity distance
～1.5 Gpc

Redshift z～0.28

初代星BBHの観測レート

Detection rate of the inspiral and QNM (a/M=0.70) by 2nd generation detectors

$$N \sim 180 \left(\frac{SFR_p}{10^{-2.5}}\right)\left(\frac{f_b/(1+f_b)}{0.33}\right) \mathrm{Err_{sys}}\ [\mathrm{yr^{-1}}]$$

SFRp is the peak value of Pop III SFR ($10^{-2.5}$ Msun/yr/Mpc^3, de Souza et al. 2011),
f_b is the initial binary fraction (1/2, Susa et al.2014),
$\mathrm{Err_{sys}}$ = 1 corresponds to adopting distribution functions and the binary evolution for Pop I stars.

To evaluate the robustness of the mass distribution and the range of $\mathrm{Err_{sys}}$, we examine the dependence of the results on the unknown parameters and the initial distribution functions.

Errsys (Example)

	Errsys
Standard	1 (180 /yr)
Mass range: ($10\ M_\odot < M < 100\ M_\odot$ or $140\ M_\odot$)	1~3.4
IMF:Flat, M^{-1}, Salpeter	0.42~1
IEF:f(e)∝e,const.,$e^{-0.5}$	0.94~1
BH natal kick: V=0,100,300 km/s	0.2~1
CE:αλ=0.01,0.1,1,10	0.21~1
Mass transfer (mass loss fraction): β=0, 0.5, 1	0.67~1.3
Worst	0.046

- 一方で 初代星BBHの典型的な質量は変わらない (~30 Msun).

なぜ初代星が 30MsunのBBHになるのか？

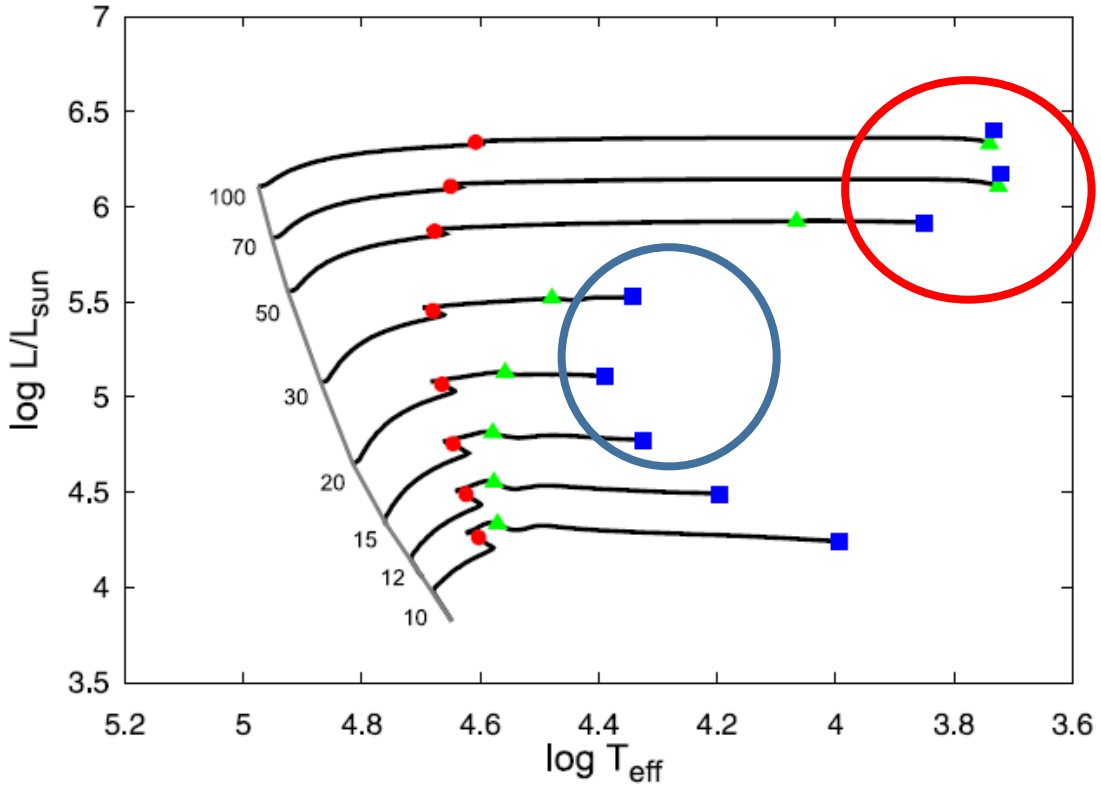

Figure 1. The Hertzsprung-Russell (HR) diagram for the Pop III stars of mass 10 $M_\odot \leqslant M \leqslant 100\ M_\odot$ using the data taken from Marigo et al. (2001). The number attached to each solid curve is the mass of each star in unit of $M_\odot$. The dashed line shows the ZAMS (Zero Age Main Sequence) stars. Red circles, green triangles and blue squares correspond to the beginning of He-burning, the end of the He-burning and the beginning of the C-burning, respectively.

- M>50Msun　赤色巨星
  →Mass transfer 不安定
  →common envelope
  →1/3~1/2 of initial mass (~25-30Msun)

- M<50Msun　青色巨星
  →Mass transfer 安定
  →mass loss が効きづらい
  →2/3~1 of initial mass (25-30Msun)

Pop III　連星進化（例）

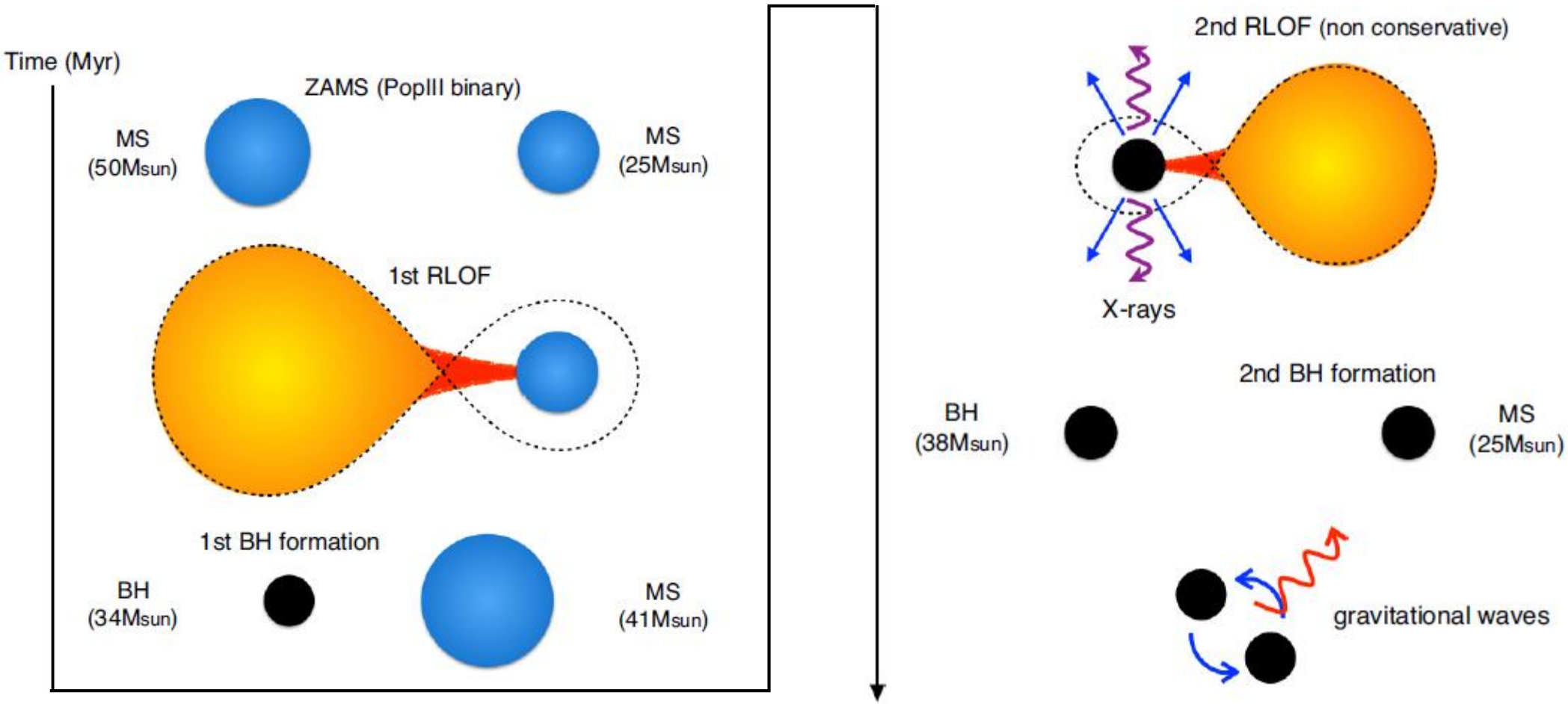

初代星 BBH

- Errsys=0.046~4

  ⇒観測レート R～8.3-720 $\left(\frac{SFR_{peak}}{10^{-2.5}}\right)\left(\frac{f_b/(1+f_b)}{0.33}\right)$ [yr^{-1}](S/N>8)

- 質量　**M～30 M$_\odot$**

初代星起源のBBHが重力波で見える（見えた?）かもしれない

1. 初代星起源のBBHではQNMも見えるかもしれない
   → 初代星起源BHからのQNMでGRの検証ができるかもしれない
2. BBHの質量分布から初代星起源を種族I,IIと区別できるかもしれない
   →初代星の検証

future plan of GW observer : B-DECIGO and DECIGO

- DECIGO: Japanese space gravitational wave observatory project
- B-DECIGO: test version of DECIGO

- B-DECIGO : z~10 (30 Msun BH-BH)
  ~10^5 events/yr
- DECIGO can see Pop III BH-BHs when Pop III stars were born! (Nakamura, Ando, TK et al. 2016)

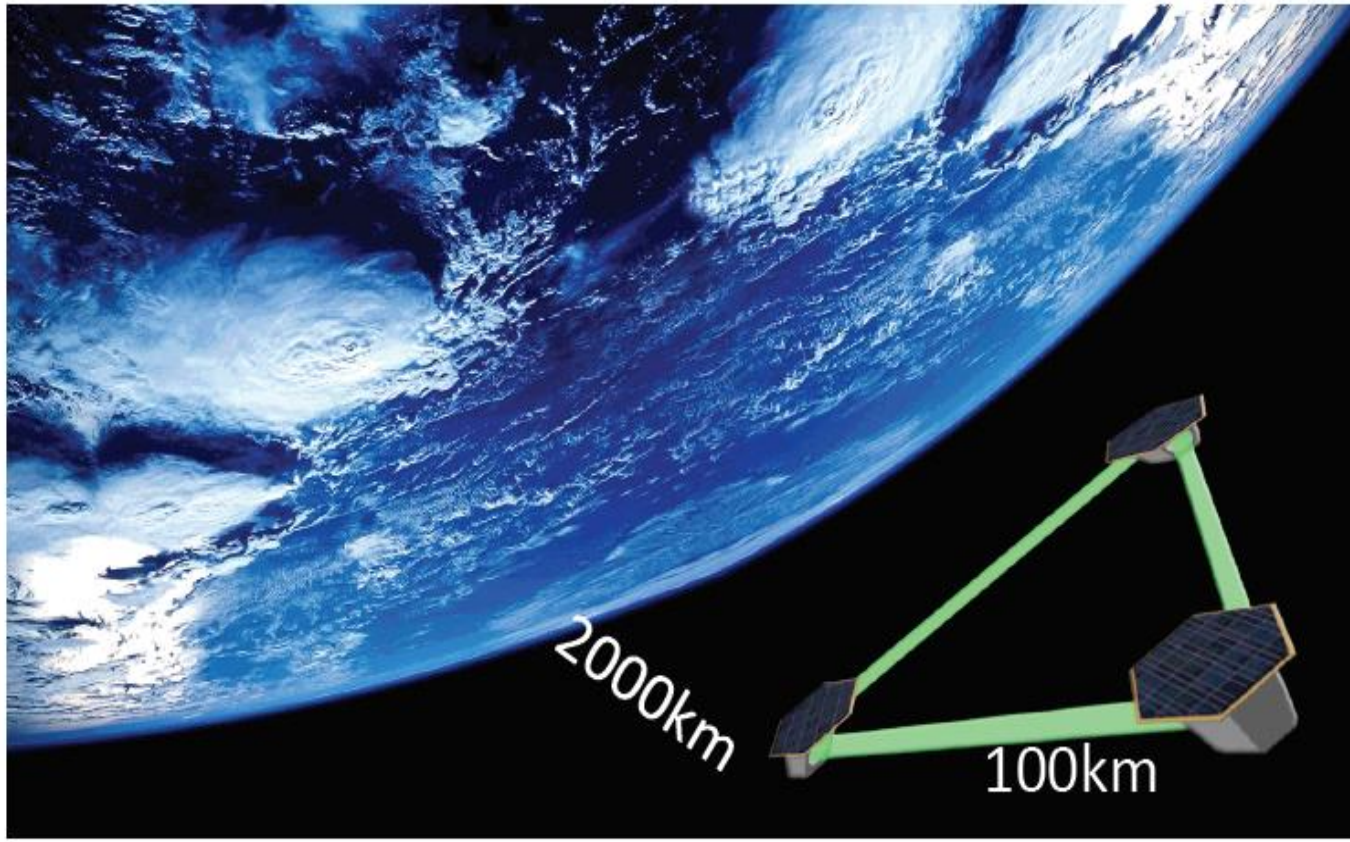

©Nakamura

Cumulative BBH merger rate

aLIGO ~10^2-10^3/yr

Pre-DECIGO ~10^5/yr

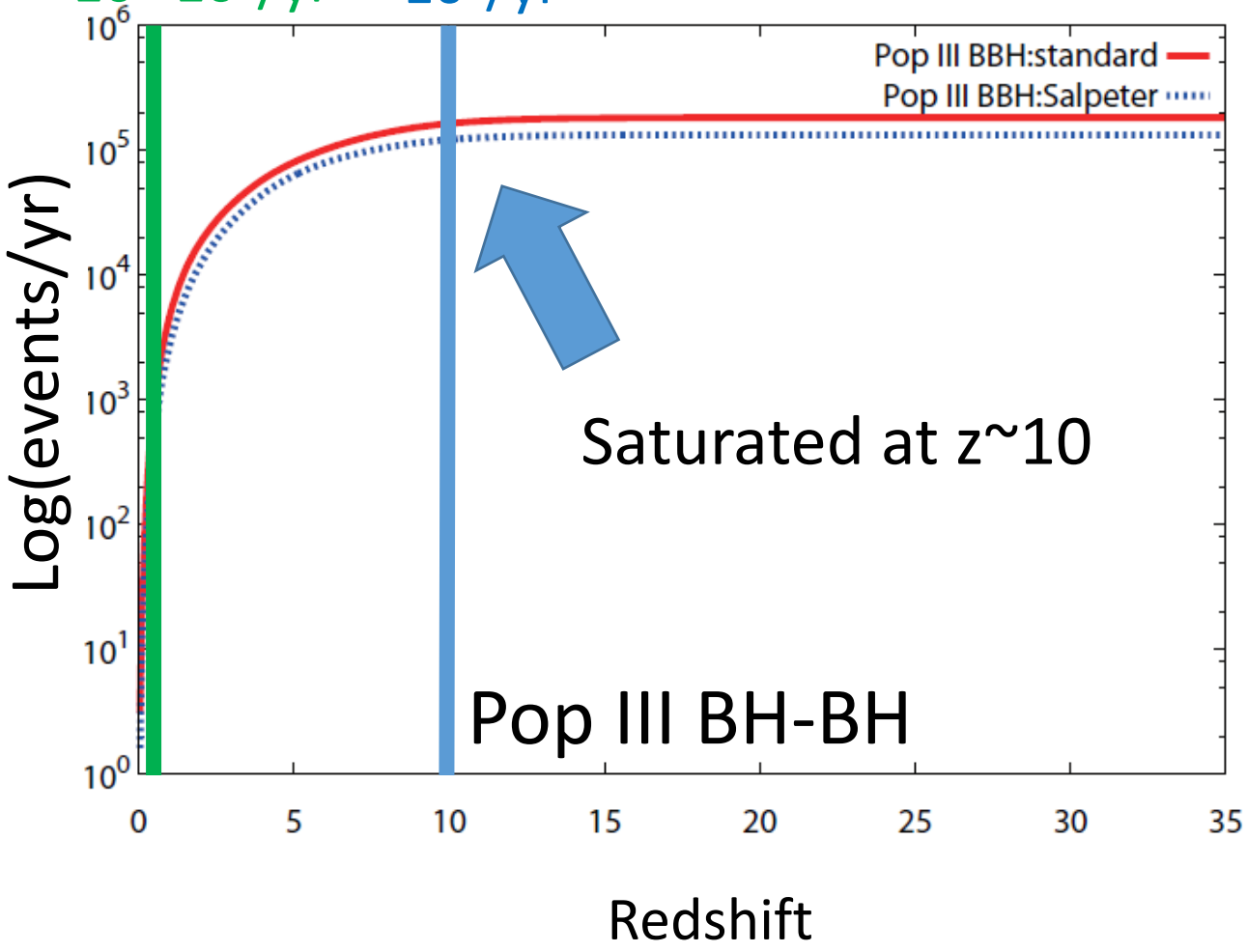

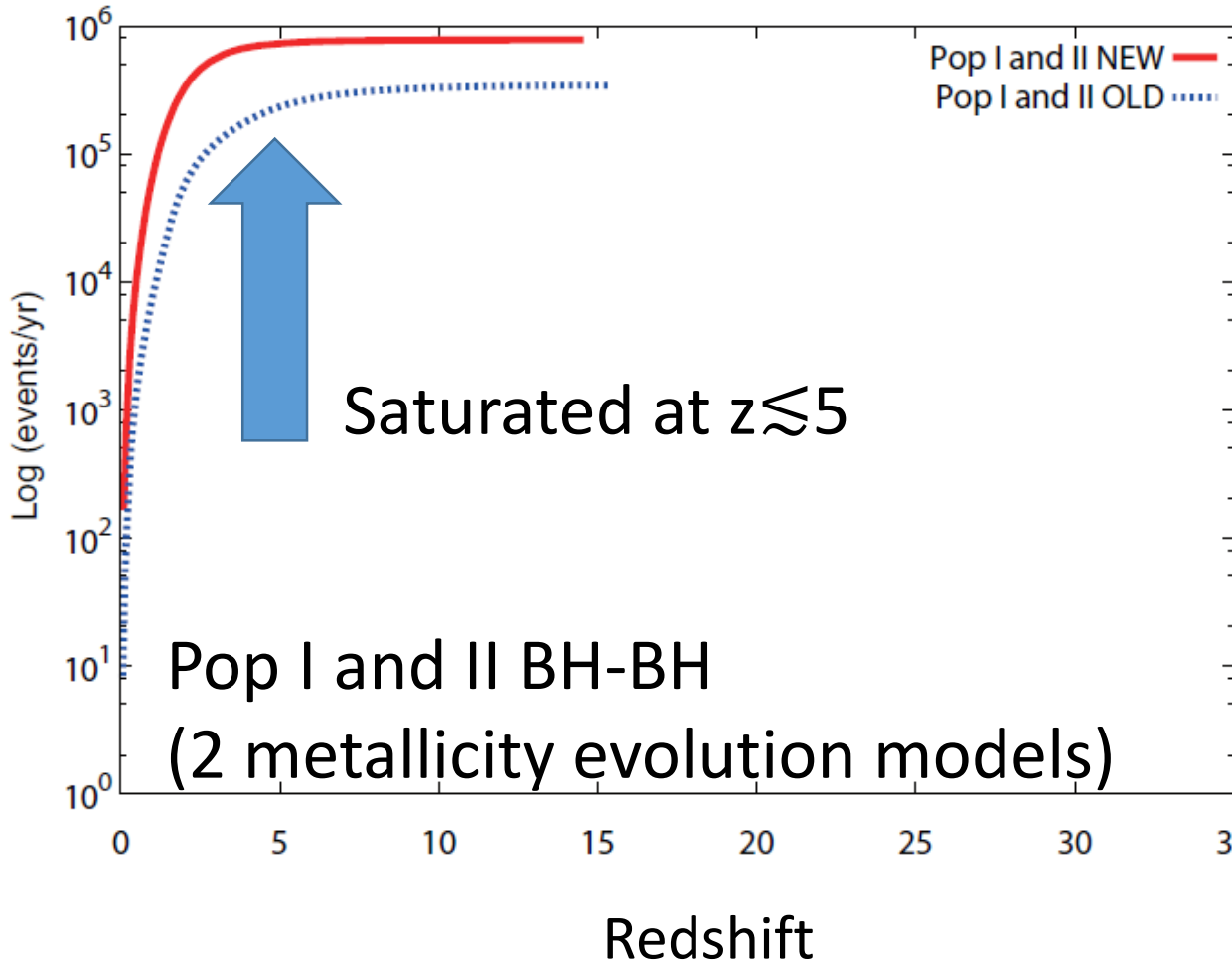

Conclusion

- 初代星は典型的に 30Msun+30Msun BBHになる
- **Detection rate of aLIGO**

$$\mathbf{R\sim 8.3\text{-}720\left(\frac{SFR_{peak}}{10^{-2.5}}\right)\left(\frac{f_b/(1+f_b)}{0.33}\right)\ [yr^{-1}\ ]}(S/N>8)$$

- 質量分布、赤方偏移分布から初代星を種族I,IIと区別可能
- DECIGOでは初代星が形成されている現場からの重力波を観測可能

SKAがらみ

- HMXBとしてX線の供給による再電離への寄与

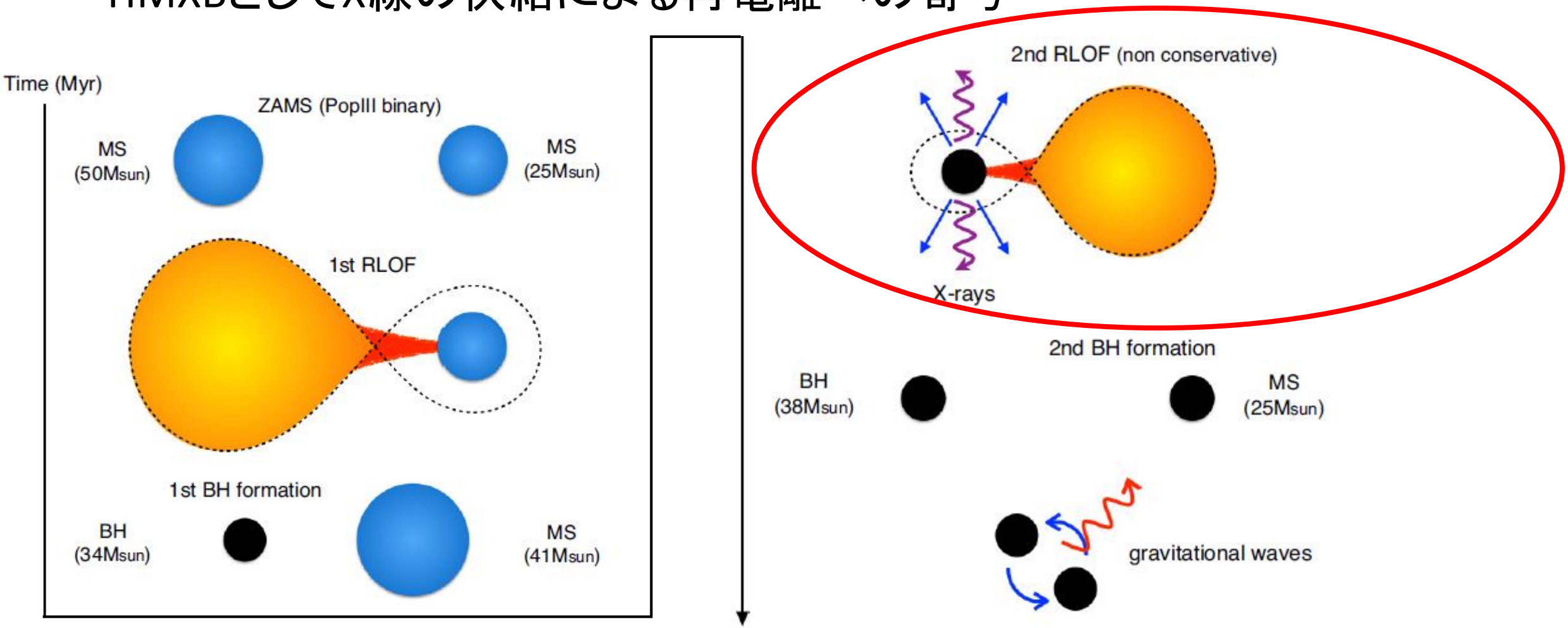

X線放射率

$$\mathcal{L}_{\rm X} \simeq 1.7 \times 10^{38}\ {\rm erg\ s^{-1}\ Mpc^{-3}} \left(\frac{f_{\rm MT}}{0.3}\right) \times \left(\frac{\epsilon}{0.05}\right) \left(\frac{\Delta M}{2\ {\rm M_\odot}}\right) \left(\frac{R_{\rm BBH}}{100\ {\rm Gpc^{-3}\ yr^{-1}}}\right)$$

$$\zeta_{\rm X} = \frac{f_{2-10}\mathcal{L}_{\rm X}}{\langle h\nu_0\rangle \dot{\rho}_{\star,{\rm III}}},$$

$$\simeq 1.2 \times 10^{57}\ {\rm M_\odot^{-1}} \left(\frac{f_{2-10}}{0.5}\right) \left(\frac{\langle h\nu_0\rangle}{2\ {\rm keV}}\right)^{-1} \times \left(\frac{f_{\rm MT}}{0.3}\right) \left(\frac{\epsilon}{0.05}\right) \left(\frac{\Delta M}{2\ {\rm M_\odot}}\right).$$

- 天文月報10月号に詳しく書いてます
- http://www.asj.or.jp/geppou/contents/2016_10.html
- 重力波無料本公開中
- http://www.gw.hep.osaka-cu.ac.jp/GRforPublic/

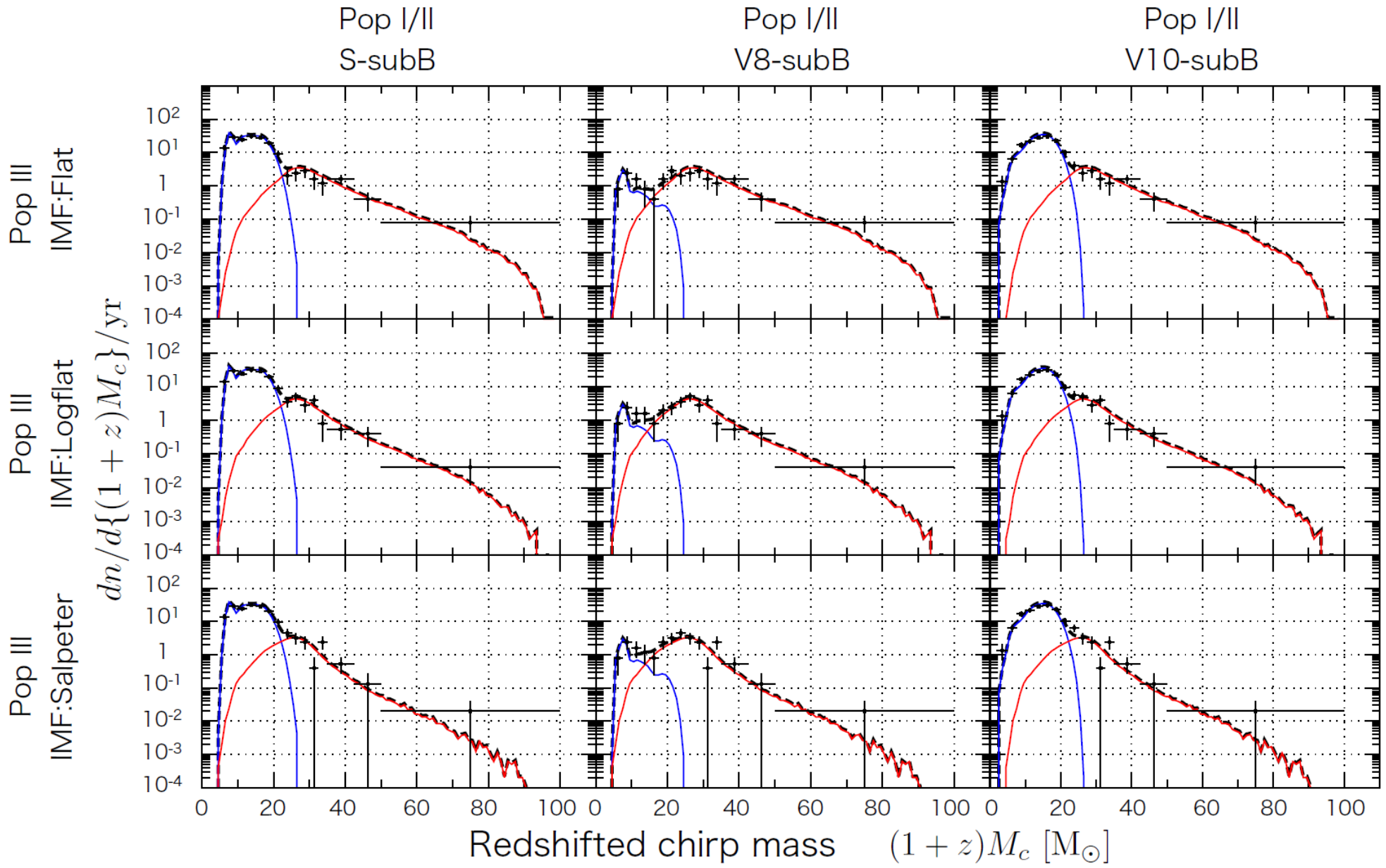

Miyamoto et al. in prep.

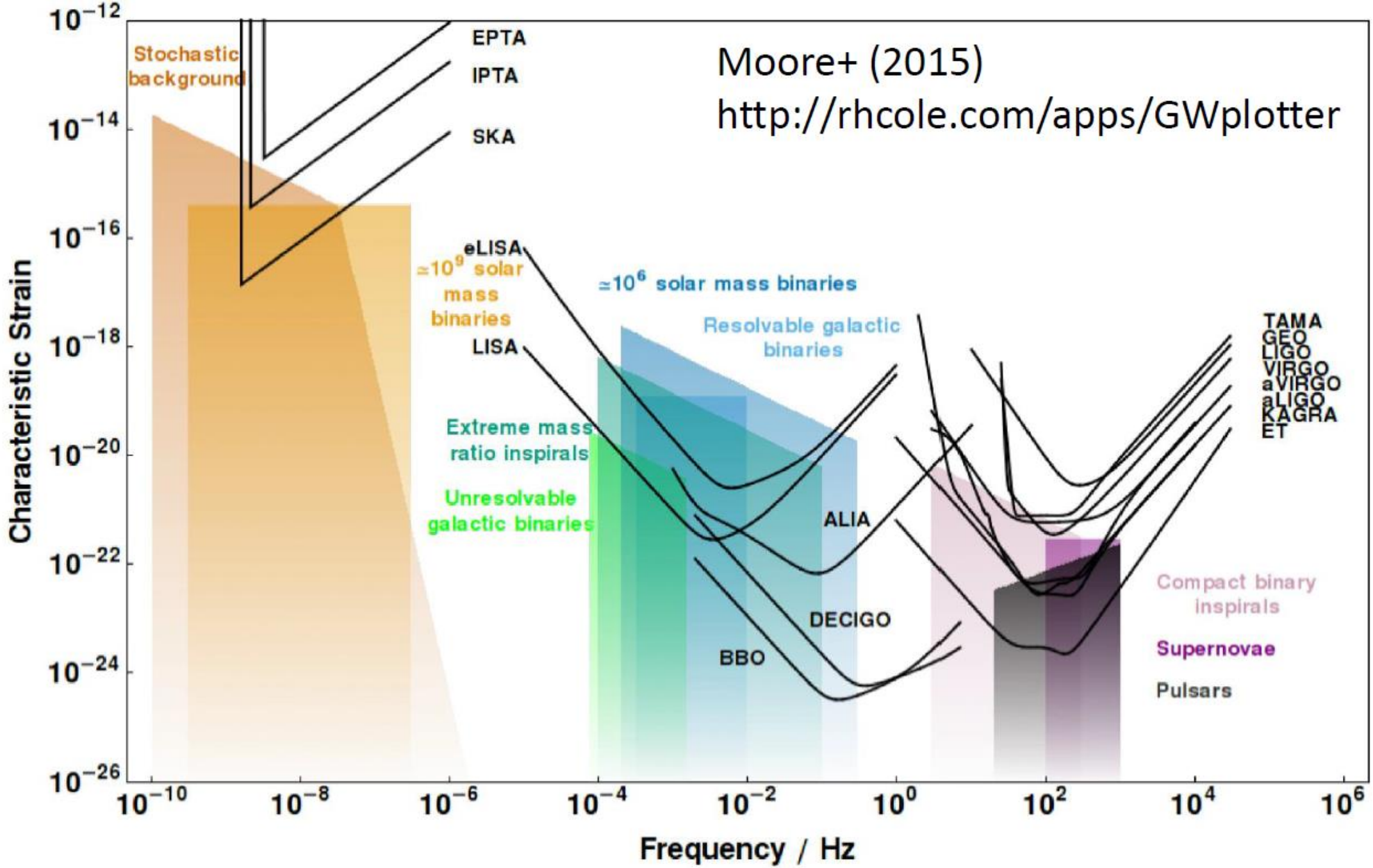
Moore+ (2015)
http://rhcole.com/apps/GWplotter
Stochastic background
EPTA
IPTA
SKA
eLISA
≃10^9 solar mass binaries
LISA
≃10^6 solar mass binaries
Resolvable galactic binaries
Extreme mass ratio inspirals
Unresolvable galactic binaries
ALIA
DECIGO
BBO
TAMA
GEO
LIGO
VIRGO
aVIRGO
aLIGO
KAGRA
ET
Compact binary inspirals
Supernovae
Pulsars
Characteristic Strain
Frequency / Hz
10^-12
10^-14
10^-16
10^-18
10^-20
10^-22
10^-24
10^-26
10^-10
10^-8
10^-6
10^-4
10^-2
10^0
10^2
10^4
10^6

Other Pop III SFRs

- SPH simulation
  (Johnson et al. 2013)
  SFRp~ 10^{-3}-10^{-4} Msun/yr/Mpc^3
- Constraints by Planck
  (e.g.Hartwig et al.2016, Inayoshi et al.2016)
  optical depth of Thomson scattering
  total Pop III density$\lesssim 10^{4\text{-}5}$ Msun/Mpc^3
  by Visbal et al.2015

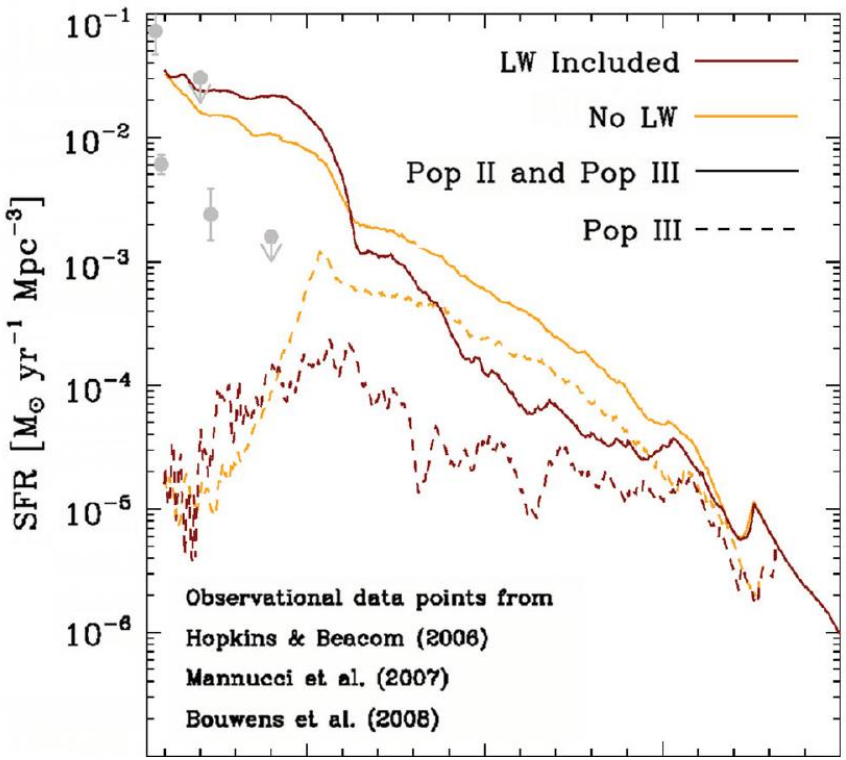

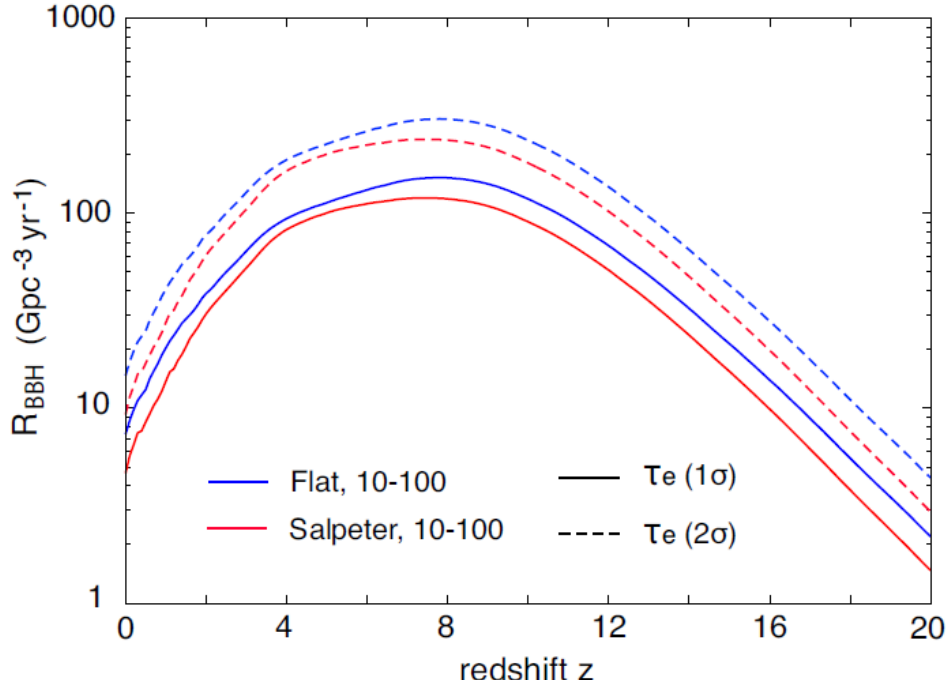

The treatment of CE

- We assume the fraction of the orbital energy is used to expel envelope.
- We use simple energy formalism in order to calculate separation after CE a_f

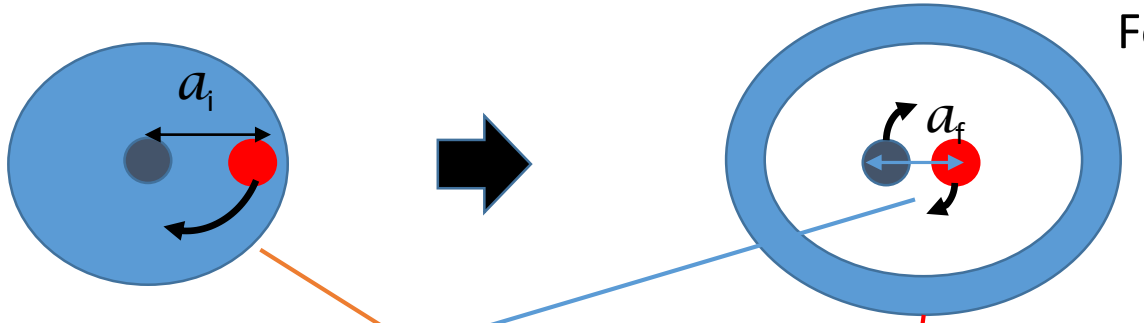

For given Mcore1, Menv1 M2, initial separation a_i

Assuming efficiency of mass ejection

Final separation a_f

$$\alpha\left(\frac{GM_{c1}M_2}{2a_f}-\frac{GM_1M_2}{2a_i}\right)=\frac{GM_1M_{env1}}{\lambda R_1}$$

The loss of orbital energy

the energy required to expel envelope

α: the efficiency of energy transfer from orbit to envelope

λ: the binding energy parameter

These common envelope parameters are uncertain.

- How much the orbital energy can be used to expel envelope?
- How much the internal energy of envelope is used to expel envelope?

The rate dependence on CE parameters

$$\alpha\left(\frac{GM_{c1}M_2}{2a_f}-\frac{GM_1M_2}{2a_i}\right)=\frac{GM_1M_{env1}}{\lambda R_1}$$

The loss of orbital energy

the energy required to expel envelope

- Separation after CE a_f is dependent on CE parameters.

For simplicity, α=1.

If λ is large i.e, the energy required to expel envelope is small,

the loss of orbital energy during CE becomes small and a_f is large.

- If a_f is large, binary tend not to merge during CE and can survive.
- However, if a_f is too large, binary cannot merge within Hubble time due to GW.

λ ↗

a_f ↗

⇒

- The number of merger during CE ↘ ⇒ Merger rates ↗
- Merger timescale $t_{GW} \propto a^4$ ↗ ⇒ Merger rates ↘

The dependence on CE parameters

For example, we consider how Pop I NS-NS merger rate depend on CE parameters.

Pop I NSNS merger rate [Myr^{-1} $galaxy^{-1}$] Dominik et al.2012

parameter	NS-NS merger rate [events/yr/galaxy]
$\alpha\lambda = 0.01$	0.4
$\alpha\lambda = 0.1$	11.8
$\alpha\lambda = 1$	48.8
$\alpha\lambda = 10$	20.8

αλ ↗

a_f ↗

- The number of coalescence during CE ↘ ⇨ Merger rates ↗
- Merger timescale $t_{GW} \propto a^4$ ↗ ⇨ Merger rates ↘